ASSESSMENT OF CLIMATE CHANGE IMPACT ON SURFACE WATER RESOURCE IN WOSHA WATERSHED, RIFT VALLEY LAKES BASIN, ETHIOPIA

M.Sc. THESIS

ELSAE WARE GIDESA

HAWASSA UNIVERSITY, HAWASSA, ETHIOPIA

OCTOBER, 2024

ASSESSMENT OF CLIMATE CHANGE IMPACT ON SURFACE WATER RESOURCE IN WOSHA WATERSHED, RIFT VALLEY LAKES BASIN, ETHIOPIA

ELSAE WARE GIDESA

A THESIS SUBMITTED TO

THE DEPARTMENT OF HYDRAULIC AND WATER RESOURCES ENGINEERING,

FACULTY OF BIOSYSTEMS AND WATER RESOURCES ENGINEERING,

INSTITUTE OF TECHNOLOGY, SCHOOL OF GRADUATE STUDIES

HAWASSA UNIVERSITY

HAWASSA, ETHIOPIA

IN PARTIAL FULFILLMENT OF THE

REQUIREMENTS FOR THE

DEGREE OF

MASTER OF SCIENCE IN HYDRAULIC ENGINEERING

OCTOBER, 2024

ADVISORS' APPROVAL SHEET

SCHOOL OF GRADUATE STUDIES

HAWASSA UNIVERSITY ADVISORS' APPROVAL SHEET

This is to certify that the thesis proposal entitled **"**ASSESSMENT OF CLIMATE CHANGE IMPACT ON SURFACE WATER RESOURCE IN WOSHA WATERSHED, RIFT VALLEY LAKES BASIN, ETHIOPIA**"** submitted in partial fulfillment of the requirements for the degree of Master's with specialization in Hydraulic Engineering, Department of Hydraulic and Water Resource Engineering, and has been carried out by ELSAE WARE GIDESA ID. No. GpHyW/0003/13 under our supervision Therefore, we recommend that the student has fulfilled the requirements and hence hereby can submit the thesis proposal to the department

Abebe Tadesse (PhD)	____________________	________________
Name of Major Advisor	Signature	Date
Petros Yohannes (M.Sc.)	____________________	________________
Name of the Co-advisor	Signature	Date

EXAMINERS' APPROVAL SHEET

SCHOOL OF GRADUATE STUDIES

HAWASSA UNIVERSITY EXAMINERS' APPROVAL SHEET

We, the undersigned, members of the Board of Examiners of the final open thesis proposal Defense by **Elsae Ware** have read and evaluated his thesis proposal entitled **"**ASSESSMENT OF CLIMATE CHANGE IMPACT ON SURFACE WATER RESOURCE IN WOSHA WATERSHED, RIFT VALLEY LAKES BASIN, ETHIOPIA**.",** and examined the candidate. This is, therefore, to certify that the thesis proposal has been accepted in partial Fulfillment of the requirements for the degree

.

Abebe Tadesse (PhD)	______________	___________
Name of Major Advisor	Signature	Date
______________________	______________	___________
Name of Internal Examiner-I	Signature	Date
Tewodros Meless (PhD)	______________	Dec.18, 2014
Name of Internal Examiner-II	Signature	Date
Fikru Fentaw (PhD)	______________	Dec.12,2024
Name of External Examiner	Signature	Date
____________________	____________	__________
SGS Approval	Signature	Date

DECLARATION

I hereby declare that this MSc Specialty or equivalent thesis is my original work and I have not seen this thesis presented in this university for a degree/ in any other university, and all sources of material used for this thesis have been duly acknowledged.

Name: ELSAE WARE GIDESA

Signature________________

Date________________

DEDICATION

This Thesis is dedicated to my Mother Warite Elale. Hato, you are the main reason for being who I am.

ACKNOWLEDGMENTS

In all humility I bow before God, the compassionate and the most merciful who bestowed me with the heart to feel and brain to think and complete this thesis.

Next, I would like to sincerely thank **Dr. Abebe Tadesse**, my adviser, for all of his help and support during my thesis research. His knowledge, perceptions, and criticism have greatly influenced my studies. I am appreciative of his desire to impart his expertise as well as the time and energy he has put into helping me succeed academically.

I am highly indebted to my Co- advisor **Mr. Petros Yohannes,** for all the support and guidance He has extended to me during my study. I do not think that I would have reached this stage without your genuine advice. He is very supportive, willing, and generally great.

Additionally, I owe a debt of gratitude to the employees at Hawassa University's Hydraulics and Water Resources Engineering department as well as the Technology Institute for supporting and facilitating my post-graduate coursework and thesis work.

I would not like to forget thanking my family for their steady support has been showing me from the beginning to this moment. Their encouragement has given me energy and made me efficient whereas others who supported me include my friends who have also offered unwavering help. They were all patient enough to understand whenever I put research first before attending to anything else.

TABLE OF CONTENTS

LIST OF TABLES

LIST OF FIGURES

ABBREVIATIONS/ACRONYMS

CANESM5	Second Generation Canadian Earth System Model
CC	Climate Change
CMhyd	Climate model for hydrologic modeling
CMIP6	Coupled Model Intercomparison Project Phase 6
DEM	Digital Elevation Model
GCMs	Global Climate Models
GHGs	Greenhouse Gases
GIS	Geographic Information System
IPCC	Intergovernmental Panel on Climate Change
ITCZ	inter-tropical convergence zone
LULC	Land Use Land Cover Change
MIROC6	Model for Interdisciplinary Research on Climate, Version 6
MOWE	Ministry of Water and Energy
NESM3	Nanjing University of Information Science and Technology Earth System Model, Version 3
NMAE	National Meteorological Agency of Ethiopia
RCP	Representative Concentration pathways
SSPs	Shared Socioeconomic Pathways
SWAT	Soil and Water Assessment Tool
USGS	United States Geological Survey

ABSTRACT

Climate change (CC) and Land Use/Land Cover (LULC) changes present significant threats to global water resources and socio-economic systems. This study aimed to evaluate the impact of climate change and LULC changes on the availability of surface water resources in the Wosha watershed, located in the Rift Valley Lakes Basin (RVLB) of Ethiopia. The available water resources were assessed using the Soil and Water Assessment Tool (SWAT), a semi-distributed, physically-based hydrological model. Calibration and validation of computed stream flow were conducted using SWAT-CUP with the SUFI-2 algorithm. Bias-corrected data from three climate models output from Coupled Model Intercomparison Project Phase 6 (CMIP6) models such as CANESM5, MIROC6, and NESM3 were used to assess baseline (1985-2014), mid-term (2041-2070), and long-term (2071-2100) periods under the Shared Socioeconomic Pathways (SSP2 4.5 and SSP5 8.5) climate scenarios. The SWAT model's performance was robust, achieving R^2 values of 0.88 and NSE values of 0.75 during calibration, and R^2 values of 0.83 and NSE values of 0.72 during validation for monthly simulations. The projections indicate that both rainfall and temperature will increase under SSP2 4.5 and SSP5 8.5 scenarios in the mid-term period, with a temperature rise of 1.2°C expected under SSP5 8.5. Precipitation is also expected to increase by 1% to 10% in the long term for both scenarios. Therefore, the primary objective of this study was to assess the impact of climate and LULC changes on the availability of surface water resources in the Wosha watershed. The results underscore the importance of understanding surface water availability and mitigating the impact of climate change to ensure future water resources for the region.

Keywords: Climate Change; CMIP6; Copernicus; Wosha watershed; SSP; SWAT-CUP; Water Availability

1. INTRODUCTION

1.1. Background

Climate change refers to the long-term patterns of atmospheric conditions (Boru et al., 2019). While it can change over time, human activities such as burning fossil fuels and deforesting have accelerated these changes in recent decades. These activities have increased greenhouse gas (GHG) levels in the atmosphere, trapping heat and causing the Earth's temperature to rise. The impact of climate change on the hydrology of the globe is observed in different basins of the world. The hydrology of Africa is shaped by complex interactions between the atmosphere, land, and ocean. Freshwater availability is highly seasonal and influenced by both local and distant rainfall patterns, resulting in significant variability across the continent.

Surface water is a crucial resource for sustaining life on Earth (Von Uexkull & Buhaug, 2021). It supports ecosystems in lakes, rivers, and wetlands and provides essential water for human use. Surface water also plays a vital role in global water and climate cycles. Variations in surface water extent affect these global cycles and impact water resource availability, which has significant implications for both human societies and ecosystem sustainability. In Ethiopia, climate change poses a serious threat to surface water resources. The country's dependence on unpredictable annual rainfall makes it highly vulnerable to water scarcity. Climate change is exacerbating this problem, intensifying the challenges of water security. Effective and sustainable management of water resources requires addressing the impacts of climate change.

Climate change represents a significant threat to global water resources, impacting both the availability and quality of surface water. In regions like the Rift Valley Lakes Basin in Ethiopia, the effects of climate change are becoming increasingly evident, manifesting in altered precipitation patterns, shifts in temperature, and intensified hydrological extremes. These changes have profound implications for water resource management, agricultural productivity, and ecosystem sustainability.

The Wosha watershed, a critical component of the Rift Valley Lakes Basin, exemplifies the vulnerability of surface water resources to climate variability. This watershed, characterized by its unique hydrological and ecological attributes, has experienced noticeable changes in recent decades. According to recent studies, shifts in rainfall patterns and increased temperatures have led to significant alterations in stream flow regimes and water availability in this region (Tadese et al., 2020). The resultant hydrological stress not only affects local communities but also threatens the broader ecological balance of the basin.

Assessing the impact of climate change on surface water resources in the Wosha watershed is crucial for developing effective adaptation and management strategies. Understanding these impacts can help in formulating policies that mitigate adverse effects and enhance the resilience of both human and natural systems. This study aims to provide a comprehensive evaluation of these impacts, focusing on changes in precipitation, temperature, and their implications for surface water dynamics in the Wosha watershed.

This study was used SWAT model to simulate surface water availability under climate change to understand changes in baseline (1985-2014), mid-term (2041-2070), and long-term (2071-2100) periods under SSPs. Climate Model for Hydrological model (CMhyd) tool was applied to reduce bias from climate models. The fundamental objective of this study is to assess the impact of climate change on water availability in Wosha watershed RVLB, Ethiopia.

1.2. Statement of the Problem

Water is a vital resource for sustaining ecosystems, agricultural activities, human consumption, and industrial processes (Edamo, Bushira, et al., 2022). The availability of surface water is particularly crucial in regions like Ethiopia's Rift Valley Lakes Basin (RVLB), where agriculture dominates the economy and livelihoods. In recent years, the Wosha watershed within the RVLB has experienced significant environmental changes, which are exacerbating the already complex issues related to water availability. These changes, driven by climate variability, land use alterations, and population growth, pose substantial challenges to the sustainability of water resources in the region (Ukumo, Edamo, et al., 2022).

Despite the critical importance of water resources in the Wosha watershed, there is a noticeable gap in the literature regarding a comprehensive assessment of surface water availability in this specific area. Globally, numerous studies have examined the impacts of climate change on water resources, with findings indicating significant reductions in surface water availability, altered hydrological cycles, and increased frequency of extreme weather events (Boru et al., 2019; Edamo, Bushira, et al., 2022; Orke & Li, 2021; Ukumo, Edamo, et al., 2022). However, these studies often focus on larger watersheds or global models that may not capture the nuances of smaller, regional watersheds like Wosha watershed. Consequently, there is limited understanding of how global climate models translate to local impacts, particularly in under-researched areas like the Wosha watershed.

Moreover, while global literature has addressed the implications of climate change on water resources in various parts of the world, there is a scarcity of research that integrates local socio-economic factors with hydrological changes in Ethiopia's RVLB under Shared Socio-Economic Pathways (SSPs). The existing studies in the region often focus on Representative Concentration pathways (RCPs) on broader scales, such as the entire RVLB or other large river basins, thereby overlooking the unique characteristics and challenges faced by the Wosha watershed under SSP 4.5 and 8.5. This gap in the literature highlights the need for a focused study that assesses surface water availability in this watershed, considering both the physical and socio-economic dimensions. Understanding the specific impacts of climate change on surface water availability in the Wosha watershed is essential for developing effective water management strategies that can mitigate the potential adverse effects on agriculture, human settlements, and biodiversity. Additionally, such an assessment can provide valuable insights into the regional variations within the RVLB, contributing to more targeted and sustainable water management practices across Ethiopia.

This study seeks to fill the identified gap by providing a comprehensive assessment of surface water availability in the Wosha watershed. Doing so will contribute to the global discourse on climate change and water resources and offer practical solutions for enhancing water security in one of Ethiopia's most vulnerable regions.

1.3. Objectives of the Study

1.3.1. General Objective

The main objective of this study is to evaluate climate change impacts on surface water resources in the Wosha watershed and improve our understanding of how these changes are likely to affect these resources.

1.3.2. Specific objectives

- To evaluate the spatial and temporal distribution of rainfall and discharge in Wosha watershed
- To assess the impacts of climate change on the surface water resources in the watershed
- To identify the biophysical and socio-economic problems of the watershed

1.4. Research Questions

1. What is the spatial and temporal distribution of rainfall and discharge in Wosha watershed?

2. How much water is available in Wosha watershed under climate change?

3. What are the biophysical and socio-economic problems of the watershed?

1.5. Scope of the study

The scope of this study encompasses a detailed examination of both climatic variables and LULC changes and their combined effects on water availability in the Wosha watershed, part of the Rift Valley Lakes Basin in Ethiopia. The study involved the use of historical climate data, future climate projections, and satellite imagery to analyze changes in precipitation patterns, temperature variations, and land use dynamics over time. SWAT model was employed to simulate how these changes impact surface water with a focus on understanding the temporal and spatial distribution of water availability. By integrating climate models, LULC analysis, and hydrological assessments, this research aims to provide a holistic understanding of the future of water resources in the watershed and offer evidence-based recommendations for adaptive management strategies to mitigate adverse impacts. Due to time and resource constraints, groundwater is not considered in this study.

1.6. Significance of the Study

The effects of climate change and land use/land cover (LULC) changes on water availability are critical to understanding the sustainability of water resources in the context of a rapidly changing environment. As global temperatures rise and weather patterns become more unpredictable, the hydrological cycle is significantly altered, affecting precipitation, evapotranspiration, and runoff patterns. These changes can lead to more frequent and severe droughts or floods, directly impacting water availability. Additionally, human-induced LULC changes, such as deforestation, urbanization, and agricultural expansion, further exacerbate these effects by altering the natural infiltration and runoff processes. This study is significant because it provides a comprehensive analysis of these intertwined factors, offering valuable insights for policymakers and water resource managers to develop adaptive strategies that ensure sustainable water availability. Understanding these dynamics is crucial for maintaining ecological balance, securing water for human consumption, agriculture, and industry, and mitigating the adverse effects of climate change on vulnerable communities, particularly in regions like the Rift Valley Lakes Basin in Ethiopia, where water resources are already under stress.

1.7. Overview of thesis

The thesis contains five chapters and is organized according to guidelines. Chapter one contains the background of the study, a statement of the problem, objectives, scope, and significance of the study. Chapter two is a literature review that summarizes the previous studies regarding climate change impacts on surface water availability. Chapter Three materials and methods that describe the types of data used in this study, climate models, remote sensing images, future predictions, and models used. Chapter four represents the outcomes of the model, calibration, validation, and sensitivity analysis. Chapter Five last chapter concludes the results and give recommendations for future research.

2. LITERATURE REVIEW

2.1. Overview of Climate Change and its Effects on Surface Water Availability

Climate change refers to the changes in the Earth's temperature that humans are bringing about through the burning of fossil fuels, the clearing of forests, and other actions that raise the atmospheric concentration of greenhouse gases (GHG) (Abdollahbeigi, 2020). Climate change can be defined as a long-term, ongoing change in the range of weather conditions, such as more frequent and severe extreme storms, or as an increase or decrease in average weather conditions, such as maximum and minimum temperatures. The increased global warming, rising average temperatures, shifting rainfall patterns, widespread melting of snow and glaciers, and rising sea levels all of which have been documented for at least 30 years can be used for global climate change analysis (Kim et al., 2014).

Climate change poses a significant threat to surface water availability in the Wosha watershed. As temperatures rise and precipitation patterns become more erratic, the hydrological cycle is expected to undergo significant changes. Studies by Edamo et al. (2022) predict that the watersheds in the Rift Valley Lakes basin will experience more frequent and intense droughts, reducing the amount of water available for both ecological and human needs. The increasing frequency of extreme weather events, such as floods and droughts, further complicates water management in the watershed. According to Ukumo et al. (2022), these events can lead to sudden changes in water availability, with periods of excess water followed by severe shortages. This variability poses challenges for water storage, distribution, and allocation, particularly in a region already facing water stress (Nica et al., 2019).

2.1.1. Climate Change in Ethiopia

There are several climate change events and repercussions of climate change on the environment and human societies. There is also an emerging consensus that Eastern Africa, and particularly Ethiopia, is one of the most vulnerable countries due to its great reliance on climate-sensitive sectors, particularly in agriculture (Kundzewicz et al., 2014). Ethiopia's contribution to global greenhouse gas emissions is negligible, but it is frequently affected by the adverse impacts of climate change brought by the carbon-intensive development paths of rich countries over the past century. The annual average temperature is projected to increase by 3.84 °C compared to that of 1960- 1990 while, the average annual rainfall will reduce by 3.5% at the end of the 21st century (Dalle et al., 2023). Similarly, the trend of mean annual temperature and annual rainfall variability were observed over the country from 1951 to 2000. The result showed that there has been a warming trend in the annual temperature over the past 55 years. It has been increasing by about 0.37°C every 10 years, case of this; the country has also experienced both dry and wet years over the same period (Ukumo, Lohani, et al., 2022).

2.1.2. Climate Models

Climate models are mathematical representations of the climate system, expressed as computer codes and run on powerful computers (Pielke et al., 2022). Different kinds of climate models range from simple energy balance models to complex earth system models (Stewart-Koster et al., 2023). The General circulation model (GCM) is a mathematical description of the Earth's climate system that is broken into several grid boxes and levels in the atmosphere, ocean, and land. Each of the grid boxes serves as a model calculation unit at which equations are solved that describe the large-scale balances of the momentum, heat, and moisture (Chen et al., 2021). GCMs are the only credible tools currently available for simulating the response of global climate systems. It is standard practice to use observed data in the form of daily or monthly time series representing the current baseline period and to apply changes derived from GCM information to these observed data (30 years as a standard baseline by WMO) (IPCC, 2023b).

2.1.3. Climate Scenarios

Scenarios are indicators of how levels of emission might increase in the future and analyze how driving forces such as natural and human activities may influence emission outcomes for the future and estimate related uncertainties (Boru et al., 2019). They can help to understand the effect as well as the impact of climate change and also its adaptation and mitigation mechanism (IPCC, 2023a). A set of scenarios was developed to show the level of driving agents and emissions to reflect the present-day climate patterns, the recent past climate, and the changes of climate for long periods. It can be used to estimate future atmospheric situations for decades or centuries in the future, but never predict the local weather condition on a particular day (IPCC, 2023a).

Scenarios have long been used by climatologists and researchers to analyze and understand the effect as well as the situations in which outcomes are uncertain (Kopp et al., 2023).

A range of scenarios can be used for climate researchers, climatologists, and policymakers to make decisions and identify sensitive parameters that induce future climate change (IPCC, 2023a). These future scenarios of driving agents such as greenhouse gasses and aerosols are fed into the climate models as input, and the output of these climate models is further used in climate change analysis and hence, the assessment of impacts, effects, adaptation, and mitigation mechanisms. The scenarios from the Special Report on Emission Scenarios (Aversa, 2023) and more recently, the Shared Socioeconomic Pathways (IPCC, 2023a) are used in climate research.

2.1.4. The Representative Concentration Pathways (RCPs)

The RCPs (Representative Concentration Pathways) used in CMIP5 are a set of scenarios that describe possible future trajectories of greenhouse gas emissions and concentrations, land use, and socioeconomic factors (Tariq et al., 2023). These scenarios were developed to provide a common framework for climate modeling and to facilitate the comparison of different models' projections of future climate change (Asempah et al., 2024).

The RCPs were chosen to represent a broad range of possible future climate outcomes, from a peak and decline in radiative forcing (RCP2.6) to a continued rise in radiative forcing (RCP8.5). Each RCP has a specific level of radiative forcing by 2100, which is a cumulative measure of human emissions of greenhouse gases (GHGs) from all sources expressed in Watts per square meter. In summary, the RCPs in CMIP5 are a set of scenarios that describe different possible future trajectories of greenhouse gas emissions and concentrations, which are used to drive climate models and generate projections of future climate change.

2.1.5. The Shared Socioeconomic Pathways (SSPs)

SSPs are the most, latest climate change scenarios. The SSPs are used in the 6th IPCC Assessment Report (AR6). The implications of climate change for the environment and society will depend not only on the response of the Earth system to changes in irradiation forcing but also on how humankind responds to changes in technology, economics, lifestyle, and policy (Kc, 2024). The main reasons for developing the new SSP scenarios were as a result of SRES scenarios do not consider climate policy; the latest developments in climate models require detailed information on emissions by source type and allow consistent usage of scenarios through the collaboration of various disciplines. The new scenarios are thus intended to connect work on climate change, impacts and adaptation, and mitigation (IPCC, 2023a). Unlike Special Report on Emission Scenarios (SRES), SSPs start with pathways of radioactive forcing (the change in the balance between incoming and outgoing radiation to the atmosphere caused primarily by changes in atmospheric composition), not with detailed socioeconomic narratives or scenarios (Samir, 2024).

2.1.6. The Comparison of CMIP5 and CMIP6

The RCPs (Representative Concentration Pathways) used in CMIP5 and the SSPs (Shared Socioeconomic Pathways) used in CMIP6 are both sets of scenarios that describe possible future trajectories of greenhouse gas emissions and concentrations, land use, and socioeconomic factors (He et al., 2023). RCPs only specify the radiative forcing pathway, while SSPs also include socioeconomic narratives and challenges to adaptation and mitigation (He et al., 2023). There are 4 RCPs (RCP2.6, RCP4.5, RCP6.0, RCP8.5) that span a range of radiative forcing levels in 2100 and There are 5 SSPs (SSP1 to SSP5) that describe different socioeconomic challenges to mitigation and adaptation. Each SSP can be combined with a radiative forcing pathway to create a scenario, e.g. SSP1-2.6, SSP2-4.5, SSP3-7.0, SSP5 8.5, etc.

So, in summary, the SSPs in CMIP6 build upon the RCPs from CMIP5 by adding socioeconomic context, while still maintaining comparable radiative forcing levels. This allows for a more comprehensive exploration of the uncertainties in future climate projections.

2.1.7. Downscaling Techniques

Because of their coarse resolution, global climate models (GCMs) are unable to accurately depict important sub-grid-scale characteristics including terrain, clouds, and land use (Casanueva et al., 2016). The spatial and temporal resolution gaps between what impact assessors need and what climate modelers can currently provide are filled by using climate downscaling approaches (Keller et al., 2022). The regional and local watershed processes and the large spatial resolution of GCMs differ greatly. This scale mismatch causes a considerable problem in the assessment of climate change impact using hydrological models. Therefore, the development of downscaling techniques for extracting high-resolution climate or climate change information from relatively coarse-resolution global climate models (GCMs) should receive a great deal of attention (Yersaw & Chane, 2024).

Large spatial resolution GCM outputs can be downscaled to a finer spatial resolution using two primary methods: statistical and dynamic downscaling. The goal of dynamic downscaling is to identify a few local and large-scale climate dynamics. Higher-resolution regional climate models (RCMs), which react to GCM output, are used to achieve this. Boundary conditions, or the values at the boundaries of the RCM's spatial domain, are supplied by the GCM output. The majority of RCMs have horizontal resolutions of tens of kilometers, which allows them to include crucial details about physical topography and orography in their simulations. RCMs are often best adept at monthly or coarser timeframes in terms of temporal resolution (Paranunzio et al., 2023).

Statistical downscaling consists of modeling the relationship between GCM output and observations to produce results that are useful as inputs to sector models or for direct use in decision-making. The overall idea is to establish empirical connections between predictors and values that have been seen historically, and then use those connections to inform projections for the future. Compared to dynamical downscaling, statistical models are simpler, considerably easier to build and maintain, and require a lot less computing time (Jin et al., 2023).

2.2. Surface water resources and its availability in Ethiopia

Surface water availability in watersheds is critical for sustaining ecosystems, agriculture, and human livelihoods, especially in regions like Ethiopia, where water resources are under increasing pressure due to climate variability and anthropogenic activities. The Wosha watershed, part of the Rift Valley Lakes Basin (RVLB) in Ethiopia, presents a unique case for assessing surface water availability due to its geographical location, climatic conditions, and socio-economic dynamics. Understanding the factors influencing surface water availability in this watershed is essential for developing sustainable water management strategies (Edamo et al., 2022).

The assessment of surface water availability in the Wosha watershed of Ethiopia's RVLB is a critical area of research, given the region's susceptibility to water stress. The literature highlights the complex interplay of factors, including climate change, land use changes, and hydrological processes, that influence water availability in the watershed. To ensure sustainable water management, it is essential to adopt integrated approaches that consider the watershed's unique characteristics and the socio-economic needs of its inhabitants. Future research should focus on developing adaptive management strategies that can mitigate the impacts of climate change and human activities on the watershed's water resources.

Ethiopia is often referred to as the "Water Tower of East Africa" due to its significant water resources, including numerous rivers, lakes, and wetlands. However, the distribution of these resources is highly uneven, with the central highlands receiving most of the rainfall, while lowland areas like the RVLB experience water scarcity. According to studies by Haile et al. (2021) the variability in rainfall patterns, combined with increasing water demands from agriculture, industry, and domestic uses, has led to significant challenges in managing surface water resources.

The RVLB, which encompasses several critical watersheds, including Wosha, is particularly vulnerable to water stress due to its semi-arid climate, fluctuating rainfall patterns, and growing population. The region's hydrological cycle is complex, influenced by both natural and anthropogenic factors. Understanding these dynamics requires detailed studies on the hydrology of specific watersheds like Wosha.

2.3. Hydrological Characteristics of the Wosha Watershed

The Wosha watershed is a sub-basin within the RVLB, characterized by diverse topography and climatic conditions. It plays a crucial role in feeding into the larger water bodies of the basin, which are vital for the region's water supply. The hydrological processes within the watershed, including precipitation, evapotranspiration, infiltration, and runoff, determine the availability of surface water.

The hydrology of the Wosha watershed is influenced by both natural factors, such as topography and soil type, and human activities, including land use changes and water abstraction for irrigation. The study emphasizes the need for integrated watershed management approaches that consider these diverse factors.

In recent years, climate change has emerged as a critical factor affecting surface water availability in the Wosha watershed. Studies by Sulamo et al. (2021) indicate that changes in precipitation patterns, increased temperatures, and altered evapotranspiration rates are likely to exacerbate water scarcity in the region. These changes necessitate adaptive water management strategies to ensure sustainable water use in the watershed.

2.4. Impact of Land Use and Land Cover Changes

Land use and land cover (LULC) changes have significant implications for surface water availability in watersheds like Wosha. Deforestation, agricultural expansion, and urbanization alter the hydrological processes by increasing surface runoff, reducing infiltration, and altering the timing and quantity of water flow. According to Moges et al. (2021), these changes can lead to reduced base flow in rivers, increased sedimentation, and higher flood risks, all of which negatively impact water availability.

In the Wosha watershed, LULC changes have been driven primarily by agricultural expansion and population growth. Between 1985 and 2015, the watershed experienced significant deforestation, with forested areas decreasing by nearly 30%, while agricultural lands expanded by 40%. These changes have had profound effects on the watershed's hydrology, leading to increased surface runoff, reduced groundwater recharge, and diminished river flows during dry seasons.

2.5. Hydrological models

Hydrological models are a simplified, conceptual representation of the components of the hydrologic cycle. There are different forms of hydrological models and are primarily developed for better understanding of the hydrologic processes and prediction of hydrologic phenomena in a watershed.

2.5.1. Types of hydrological models

According to Chow et al. (1988), stochastic and deterministic models are often considered to be at the top level of the classification tree, in accordance with the way they treat the randomness of hydrologic phenomena. Stochastic models use local hydrometric data to predict flows. These models allow for some randomness that results in different outputs and based on analysis of past events, commonly rainfall and river discharge (Ahmad et al., 2001). Deterministic models generally produce a single output of runoff for a given rainfall under identical physical environments. Without going to too much detail, deterministic hydrologic models can be classified into three main categories (Cunderlik, 2003).

Lumped models: lumped hydrologic model simulation evaluated only at outlet of the basin that is without explicitly accounting for the response of individual sub-basins and parameters do not vary spatially within the basin. Parameters of lumped models often do not represent physical features of hydrologic processes and usually involve certain degree of empiricism. According to Haan et al. (1994), the impact of spatial variability of model parameters is evaluated by using certain procedures for calculating effective values for the entire basin and the most commonly employed procedure is an area-weighted average. Lumped models are not usually applicable to event scale processes. If the interest is primarily in the discharge prediction only, then these models can provide just as good simulations as complex physically based models (Beven K. , 2000). Water Balance model (WATBA), Snowmelt Runoff Model (SRM), Identification of unit Hydrograph and Components from Rainfall, Evaporation and Stream flow data (IHACRES) are examples of lumped hydrological models

Distributed models: distributed hydrological model parameters are fully allowed to vary in space at a resolution usually chosen by the user. Distributed modeling approach attempts to incorporate data concerning the spatial variation of parameters together with computational algorithms to evaluate influence of this distribution on simulated precipitation-runoff behavior. Distributed models require large amounts of data for parameterization in each grid cell (Beven, 2000). However, the governing physical processes are modeled in detail, and if properly applied, they can provide the highest degree of accuracy. For instance, HYDROTEL, MIKE11/SHE and WATFLOOD are distributed models.

Semi-distributed models: parameters of semi-distributed models are partially allowed to vary in space by dividing the basin into a number of smaller sub-basins. Semi-distributed model structures are more physically based than the structure of lumped models and less demanding input data than fully distributed models. Semi-distributed model can be grouped Kinematic Wave theory models and probability distributed models. According to Beven (2000), the Wave theory models are simplified versions of surface and/or the subsurface flow equations of physically based hydrologic models. In the case of the probability distributed models, spatial resolution is considered by using probability distributions of input parameters across the basin. Examples of semi-distributed models are SWAT (Arnold et al., 1993), HEC-HMS (US-ACE, 2001), HBV (Bergström, 1995), and TOPMODEL (Cunderllk, 2003).

2.5.2. Hydrological model selection

The choice of a suitable hydrological model depends on the function that the model needs to serve. There are several hydrological models simulating the hydrological process at different spatial and temporal scales. There are various criteria which can be used for choosing the proper hydrological model for a specific problem. Further, some criteria are also user-dependent and subjective, such as the personal preference for graphical user interface, computer operation system, input-output management and structure and clarity for users.

The selection of hydrological model taking into consideration the following four fundamental selection criteria (Cunderlik and Simonovia, 2007):

- Does the model predict the variables required by the project? (Required model outputs important to the project and therefore to be estimated by the model)

- Is the model capable of simulating single-event or continuous processes? (Hydrological processes that need to be modeled to estimate the outputs adequately)
- Can all the inputs required by the model be provided within the time and cost constraints of the project? (Availability of input data)
- Does the investment appear to be worthwhile for the objectives of the project? (Price)

For this study, SWAT model was selected since it fulfills the above criteria. Besides, the model was selected because, it is physically based, semi-distributed and belongs to the public domain, computationally efficient and it requires specific information about weather, soil properties, topography, vegetation, and land management practices occurring in the watershed and identify erosion prone areas and adopt best management practice for the watershed.

2.6.General description of SWAT model

The SWAT (Soil and Water Assessment Tool) model is one of the river basin or watershed scale model developed by United State Department of Agriculture - Agricultural Research Service (USDA-ARS) in Temple, Texas during the 1970's (Arnold et al., 1998). SWAT model is physically based, semi-distributed, and can continuously simulate stream flow, sediment yield, nutrient, pesticides and agricultural management in watersheds with varying soils, land use and management conditions over long periods of time (Neitsch, et al, 2011).

In SWAT model simulation, the specific watershed information such as hydrology, weather, topography, soil, vegetation, and land use practices are required. Based upon drainage areas of the attributes, the model divides the watershed in to a number of sub-basins. And also, the sub-basins are further divided in to a number of Hydrologic Response Units (HRUs) based on land use/ cover, soil and slope characteristics.

The hydrologic processes that can be simulated using the SWAT model contains precipitation, evapotranspiration, evaporation, surface runoff, percolation, lateral flow, ground water flow and channel routing (Arnold et al., 1998). The model routes the maximum amount of sediment in reach as a function of the peak channel velocity and estimates sediment yield for each HRU using MUSLE (Williams, 1995).

2.7.Limitations of SWAT model

SWAT model has the following limitations (Arnold et al., 1998):

- Flow and sediment routing equations used by SWAT are simplistic and the model assumes channel dimensions are static throughout the simulation (may be unrealistic since simulations may be made for 100 years or more). The simplistic description of channel bed does not account for cohesive, non-cohesive or armored channels.
- SWAT model is popular due to the multi-disciplinary coverage of processes representing the hydrology, soil science, sediment transport, crop growth, in-stream water quality and the agricultural management, but it has limitation on its non-spatial representation of the HRU inside each sub catchment.
- The user is responsible for ensuring that any physical parameters entered are correct and meaningful since model is not able to check meaningfulness of values entered by user.
- Sensitivity analysis, manual and auto-calibration tools in the SWAT model is time demanding when modeling complex catchments with several HRUs. This tool should be upgraded at least with visual and objective functional representation of the results. The SWAT-CUP tool is significant improvement for the calibration procedures, however coupling SWAT and SWAT-CUP is needed to increase the efficiency of the modeling.

2.8. Previous Studies Related to this Study

Numerous studies have examined the effects of climate change on water availability, focusing on how shifts in precipitation patterns, temperature increases, and changes in evaporation rates impact surface and groundwater resources under RCPs (Krinner et al., 2013). Research has shown that regions with existing water stress are particularly vulnerable to these changes, as they may experience further reductions in water availability based on RCPs forecasting. For instance, studies in the Mediterranean and Sub-Saharan Africa have highlighted significant decreases in rainfall and runoff, leading to reduced water levels in rivers, lakes, and reservoirs. Additionally, increased temperatures exacerbate evaporation rates, compounding the effects of reduced precipitation and further straining water resources (Folland et al., 1990). These changes are still remained vacant under SSPs.

Despite these insights, there remains a gap in the literature concerning the nuanced impacts of climate change on specific watersheds, particularly those in under-researched regions such as the Wosha watershed in Rift Valley Lakes Basin in Ethiopia. Most studies tend to generalize findings across broader geographic areas or focus on regions with more extensive data availability, leaving localized effects underexplored. Moreover, there is limited research integrating the socio-economic implications of these changes on water management practices, which are critical for developing adaptive strategies. This gap is evident in areas like the Wosha watershed, where the combined effects of climate change and human activities on water availability are not yet fully understood.

Study of Ukumo et al. (2022) was utilized a combination of down-scaled climatic data to anticipate forthcoming rainfall and capacity for evapotranspiration for the 2050s, and 2080s while employing three distinct climate circumstances: RCP2.6, RCP4.5, and RCP8.5. Subsequently, the hydrological model, SWAT2012, was used to simulate the stream flow in the basin under every climate scenario. The outcomes of this investigation indicate that the hydro meteorological attributes of the middle Abbay basin are expected to be considerably influenced by the climate change. The forthcoming precipitation is anticipated to rise in all three climate scenarios, whereas the potential evapotranspiration is estimated to increase further. As a result, an escalation in stream flow within the basin is expected, yet the degree of the escalation may differ depending on the climate scenario. Discoveries hold significant consequences for the management of water resources in the middle Abbay basin under RCP 4.5 and RCP 8.5. It is vital that those responsible for planning and policymaking consider the expected variations in precipitation, potential evapotranspiration, and stream flow to create sustainable approaches for water management. The research gap observed here is the avoidance of the new Coupled Model Intercomparison Project Phase Six (CMIP6) models under shared Socioeconomic pathways (SSPs).

The study by Edamo et al. (2022) indicated that the hydrology of the Bilate Basin is significantly affected by climate change. There is an opposite trend in stream flow for the upstream and downstream segments of the river, and climatic indices are demonstrating an upward trend, particularly for cold-month precipitation. These results have noteworthy implications for Bilate River Basin water resource management. To design sustainable water management strategies, planners and policymakers must consider the predicted changes in stream flow and precipitation. Moreover, the study discovered that the increase in stream flow in the upstream area of the Bilate River Basin is primarily due to increased precipitation during cold months. This rise in precipitation is likely a result of climate change because many parts of the world are experiencing wetter cold months. The increase in stream flow is a positive impact of climate change as it can boost water availability in the region. These variabilities aren't investigated under SSPs in Wosha watershed.

Addressing this research gap is essential for formulating effective water management strategies that consider both current and future climate scenarios. A more detailed understanding of how climate change specifically affects water availability in the Wosha watershed, for instance, would help stakeholders develop targeted interventions to enhance water security. By focusing on localized studies, researchers can provide more precise recommendations for policy and practice, ensuring that adaptation strategies are tailored to the unique environmental and socio-economic conditions of each watershed.

3. MATERIALS AND METHODS

3.1. Description of Study area

Wosha watershed is one of the tributaries in Rift Valley Lakes Basin (RVLB). It is Situated in Sidama regional state at 270 km from the capital Addis Ababa. It Lies between with latitude and longitude of 6°30'N to 7°30'N and 38°15'E to 38°45'E respectively. The watershed covers an area of 2848.3 km^2 (Figure 3.1). The elevation range of the watershed is from 1538 to 3079 a.m.s.l. The agricultural land in and around the study area is used for cultivating crops consisting of chat and sugarcane, Enset, Coffee, and Mango.

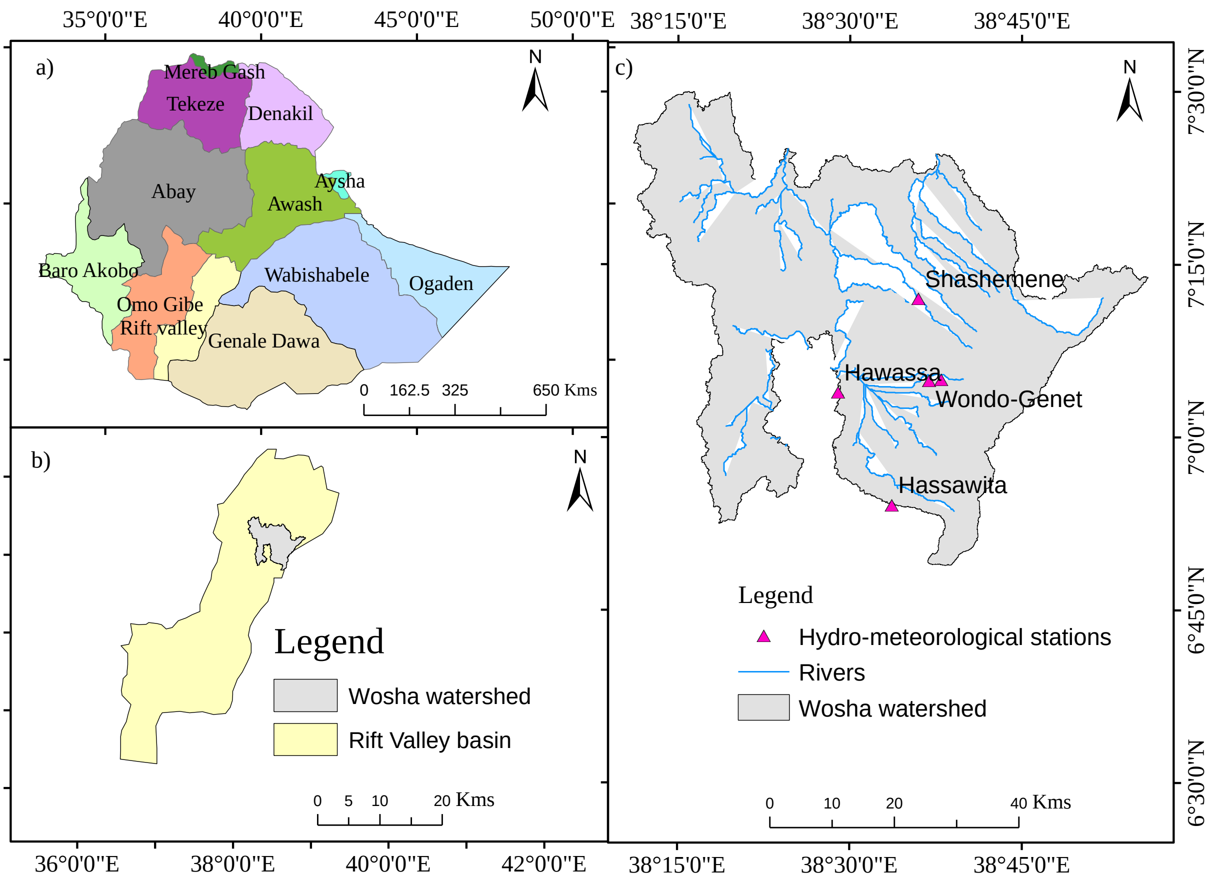

Figure 3.1: Location Map A) Ethiopia Basins B) Rift Valley Lakes Basin C) Wosha watershed

3.1.1. Hydro-meteorological property of study area

The climate characteristics of watersheds are varying from tropical to alpine (Edamo, Bushira, et al., 2022). The inter-tropical convergence zone (ITCZ) is responsible for the bimodal rainfall system bringing humid wind from the Indian Ocean. Apart from the ITCZ, the rainfall distribution in the area is affected by the effects of altitude. According to traditional classification of climate zones, with based on elevation there are five climate zones in RVLB (Table (3.1). Most of the study area is characterized by Wogna Dega and Kola especially in southern and central part of basins, also the northern and north western of part of basin is Dega and wurch. Wosha watershed has all climate zones based on the traditional classifications in RVLB because of the elevation of the watershed ranges from 1538-3079.

Table 3.1: RVLB climate zones classifications based on elevation and percentage coverages

No	Altitude range (m)	Zone	% covered
1	less than 500	Bereha	1.83
2	500 - 1500	Kola	38.06
3	1500 - 2500	Wogna Dega	50.15
4	2500 - 3000	Dega	7.50
5	3000 - 4213	Wurch	2.47

Rainfall distribution in the study area is bimodal with a long rainy season from the beginning of March to the end of May with maximum rainfall around May (300.6 mm Hawassita and 273.5 mm Hawassa). The minimum monthly rainfall is recorded in December (24.45 mm Wondo-Genet). The highest annual rainfall of the study area is recorded as 2107.2mm/year for Hassawita station. Figure 3:2 shows the continuous time series of the precipitation data in the watershed.

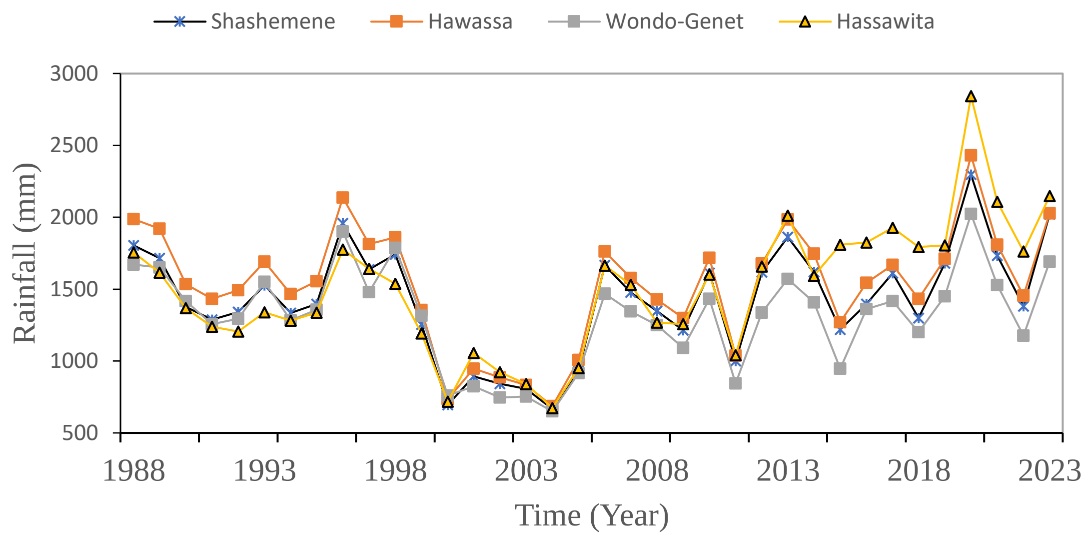

Figure 3.2: Observed Average Annual Rainfall of all Station (1988-2023)

In warm season the maximum temperature in the watershed is approximately 30°C and exceeds.

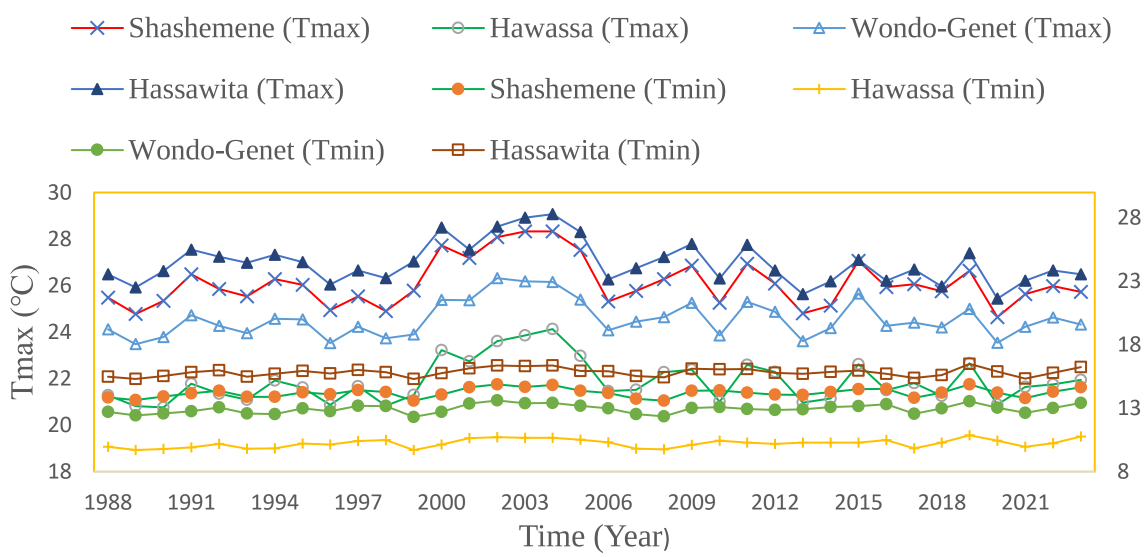

Figure 3.3: Mean Annual maximum (Tmax) and minimum (Tmin) Temperature (1988-2023)

The minimum temperature of the watershed may exceed 15℃ in January (Figure 3.3). The maximum streamflow was recorded in August (102.2m^3/s) (Figure 3.4).

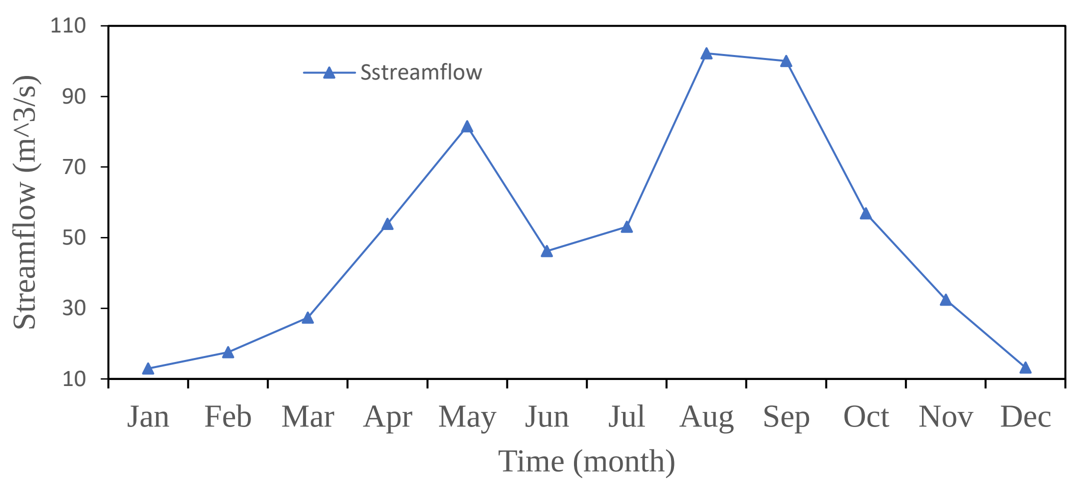

Figure 3.4: Mean Monthly flow data of Wosha watershed (2001-2015)

3.2. Data collection and analysis

A. Meteorological data

Data required as input to the SWAT model and daily observed meteorological data of rainfall, maximum and minimum temperature, humidity, sunshine hours and wind speed data used for the analysis was obtained from the National Meteorological Agency of Ethiopia (NMAE). The SWAT model required meteorological data as an input, which was the precipitation depths as a function of the return period. Meteorological stations used in this study are, Shashemene, Hawassa, Wondo-Genet, and Hassawita (Table 3.2).

Table 3.2: List of station names and locations of selected meteorological stations

SN	Station code	Latitude	Longitude	Elevation (ma.sl)
1	Shashemene	38.60017	7.200167	1927
2	Hawassa	38.48306	7.065	1694
3	Wondo-Genet	38.61556	7.082222	1742
4	Hassawita	38.56167	6.901944	2267

B. River flow data

Stream flow data was obtained from Ministry of Water and Energy of Ethiopia (MoWE). Which used for sensitivity analysis, calibration and validation of the SWAT model.

C. Climate model datasets

Table 3.3: Description of CMIP6 models used in this study

Attribute	CanESM5	MIROC6	NESM3
Full Name	Fifth Generation Canadian Earth System Model	Model for Interdisciplinary Research on Climate, Version 6	Nanjing University of Information Science and Technology Earth System Model, Version 3
Institute	Canadian Centre for Climate Modelling and Analysis (CCCma)	The University of Tokyo, Japan Agency for Marine-Earth Science and Technology (JAMSTEC), and National Institute for Environmental Studies (NIES)	Nanjing University of Information Science and Technology (NUIST), China
Resolution	Atmospheric: ~2.8° x 2.8° (T63 grid)	Atmospheric: ~1.4° x 1.4° (T85 grid)	Atmospheric: ~1.125° x 1.125° (T106 grid)

Coupled Components	Atmosphere, Ocean, Sea Ice, Land Surface, Carbon Cycle	Atmosphere, Ocean, Sea Ice, Land Surface, Carbon Cycle	Atmosphere, Ocean, Sea Ice, Land Surface
Time Periods Simulated	Historical (1850–2005), RCP Scenarios (2006–2100)	Historical (1850–2014), SSP Scenarios (2015–2100)	Historical (1850–2014), SSP Scenarios (2015–2100)
Key Features	Improved cloud schemes, better representation of the carbon cycle, coupled model with atmosphere-ocean-land-ice interaction	Advanced cloud microphysics, better aerosol processes, improved land model	Improved atmospheric convection, updated cloud schemes, interactive biogeochemistry
Primary Usage	Climate Change Projections, Carbon Cycle Feedbacks	Climate Change Projections, Earth System Interactions	Climate Change Projections, Earth System Modeling

The climate model data used were obtained from outputs of high-resolution regional climate models of CMIP6 SSPs. CMIP6 data project is formed under world climate research program (WCRP) to improve regional climate projection worldwide during sixth assessment report of IPCC. Nowadays, the CMIP6 data is applicable in most parts of the world including the African continent. For this study, only rainfall and air temperature datasets were used form climate models (Table 3.3).

D. Spatial data

Digital elevation model and Land Use/Cover (LULC) were downloaded from United States Geological Survey (USGS) earth explorer (https://earth explorer.usgs.gov/). DEM was used to delineate watershed in order to determine hydrological parameters such as, topographic map and slope map of the watershed. Land use land cover was downloaded from Landsat images for years of 1997, 2008 and 2017 (Table 3.4), because these years are cloud free years. Supervised classification with support vector machine was used to classify LULC. FAO soil data was downloaded and used in this study.

Table 3.4: LULC Images used this study

Satellite ID	**Obtaining Date**	**Resolution**	**Source**
Landsat 4-5 TM C2 L2	Jan-1-1997	30	USGS
Landsat 4-5 TM C2 L2	Jan-1-2008	30	USGS
Landsat 8-9 OLI/TIRS C2 L2	Dec-30-2017	30	USGS

3.3. Data processing and analysis

In order to construct detailed climate change scenarios for the Wosha watershed and assess their impacts on stream flow response, a hydrological model, SWAT was used.

3.3.1. Bias correction of climatic variables

Bias correction was applied to reduce overestimate or underestimate the mean of downscaled variables (i.e., temperature and precipitation) (Ayehu et al., 2018). Bias correction factors were computed from the statistics of observed and historical variables.

Distribution mapping (DM)

The DM method corrects the distribution shape of the daily precipitation based on cumulative distribution functions (CDFs) was constructed for both the observed and the SSPs simulated for all days within month. The daily precipitation for reference and future periods is obtained by Eq. (3.1) and (3.2) in terms of the Gamma CDF (F_y) and its inverse (F_{γ}^{-1}). It is also the same for temperature (Edamo, Bushira, et al., 2022).

$$P'_{ref} = F^{-1}{}_{\gamma} \left(F_{\gamma} \left(P_{ref}(d) \middle| \alpha_{ref,m} \beta_{ref,m)|} \ \alpha_{obs,m,} \beta_{obs,m}\right)\right. \quad (3.1)$$

$$P'_{fut}(d) = F_{\gamma}^{-1} \left(F_{\gamma}\left(P_{fut}(d) \middle| \alpha_{ref,m,} \ \beta_{ref,m}\right) \middle| \alpha_{obs,m,} \beta_{obs,m}\right) \quad (3.2)$$

In this research the software Climate Model Data for Hydrologic Modeling (CMhyd) was used for bias correction. It is essentially made for imagining effects of weather changes on water resources as well as hydrological systems.

3.3.2. Estimating and filling missing data

Inverse distance or weighting method is most commonly used for estimation of missing precipitation (Ly et al., 2011).

$$p_x = \frac{\sum_{i=1}^{n} \frac{P_i}{\frac{1}{D_i^{2}}}}{\sum_{i=1}^{n} \frac{1}{D_i^{2}}} \quad (3.3)$$

where, P_x=is rainfall of the missing station, n =is the number of index stations.

$$D_i^2 = \left[(x - x_i)^2 + (y - y_i)^2 \right] \tag{3.4}$$

Where D_i be the distance of the estimator station from the estimated station, x and y are the coordinates of the station whose data is estimated and x_i and y_i are the coordinates of stations whose data are used in estimation. Consistency for some stations will be tested by computing non-dimensional sing of rainfall data by dividing the monthly time series data by the average rainfall amount of the respective month (Birhanu, 2015).

$$p_i = 100x \frac{\overline{p_i}}{\overline{p}} \tag{3.5}$$

Where: p_i is the non-dimensional value of rainfall for month i, $\bar{p}_i$ is the over monthly rainfall at the station i and $\bar{p}$ is the over yearly rainfall of the station (Figure 3.5).

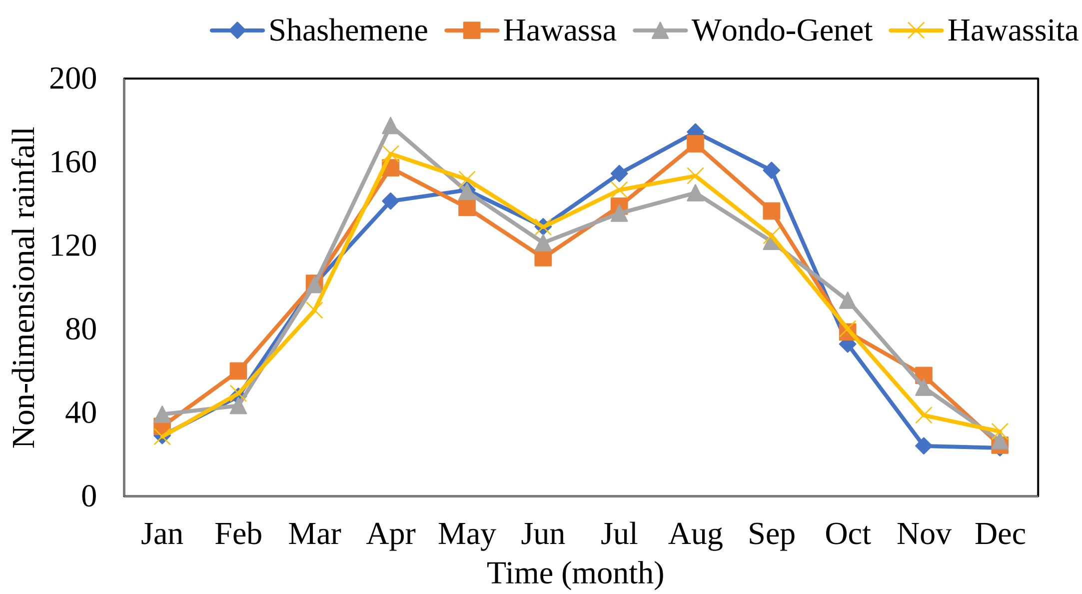

Figure 3.5: Precipitation homogeneity test

3.3.3. Checking consistency of the data

Inconsistency may result from unreported shifting of the rain gauge in gauging station. Double Mass Curve Analysis used to adjust inconsistent data (Figure 3.6). The change in the regime of the curve of the inconsistency was adjusted using Equation (3.6).

$$p_a = \frac{b_a}{a_o} x(p_o) \quad (3.6)$$

where, P_a= adjusted precipitation, p_o= Observed precipitation, b_o= Slope of graph at time $p_o$is observed, b_a= Slope of graph to which records are adjusted.

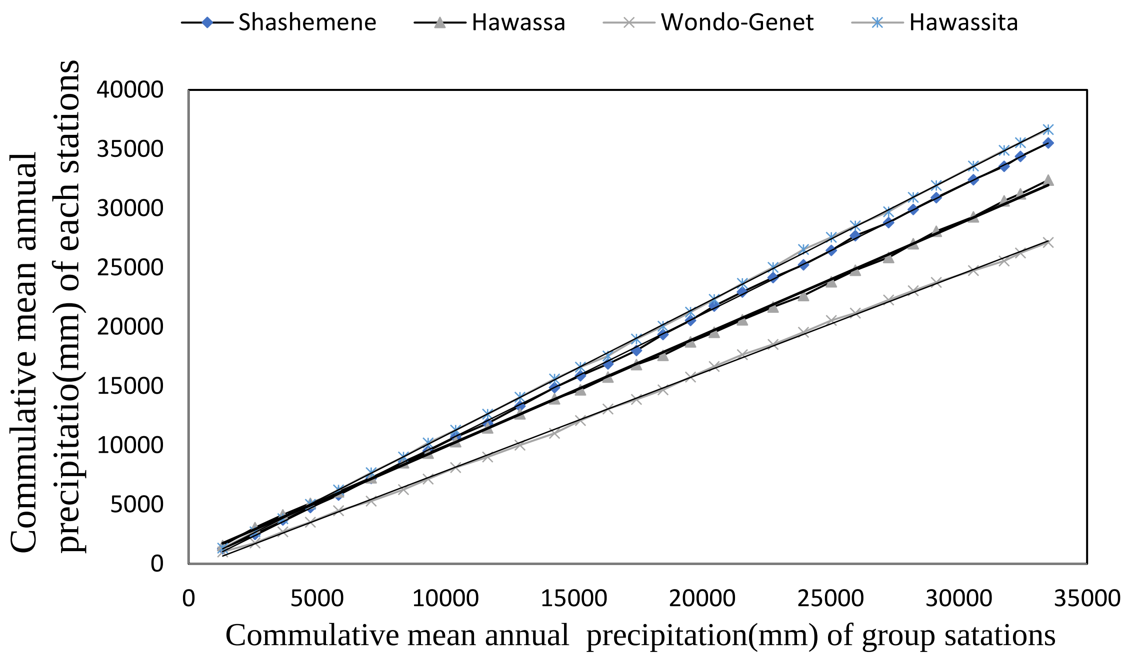

Figure 3.6: Double mass curve analysis of precipitation

Thiessen polygon method was used to calculate areal rainfall due to its simplicity to apply. This is in the principle of n-number of stations and n-polygons (Figure 3.7). The areal depth of precipitation over the total area (A) is given by:

$$\overline{P} = \frac{1}{A} x \sum_{i=1}^{n} \left(p_i x A_i \right) \quad (3.7)$$

where: $\overline{P}$ is catchment areal rainfall, p_i is Rainfall measured at station 'i',A_i: Area of subregion for stations 'i' and A is the total area of sub-regions in the catchment. Catchment areal rainfall computed was used as input to the model.

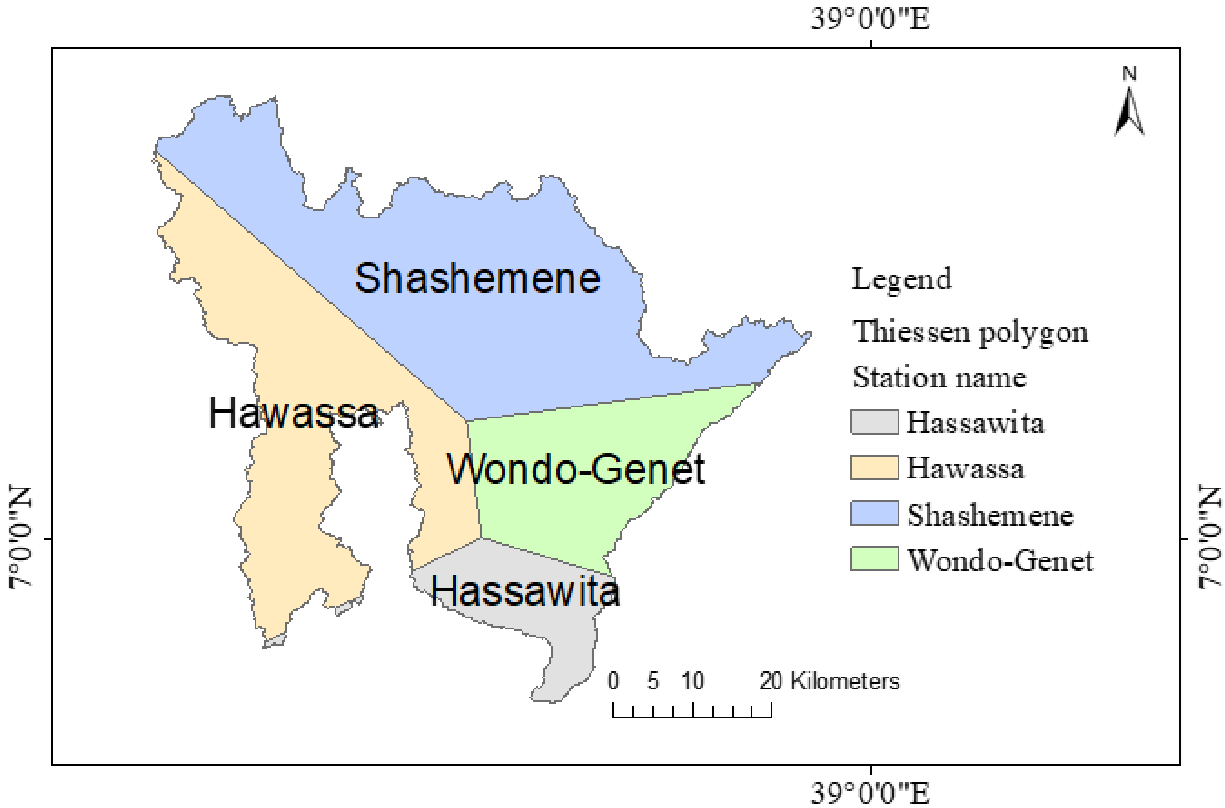

Figure 3.7: Thiessen polygon created using stations in the Wosha watershed

3.3.4. Calculation of evapotranspiration

Penman Monteith method is used to estimate Potential evapotranspiration (PET), which has been applied successfully in different parts of the world was compared with other methods and is accepted as the preferred method for computing potential evaporation from meteorological data. The FAO Penman-Monteith equation is given by:

$$ET_o = \frac{0.048\Delta(R_n - G) + \gamma \frac{900}{T+273} U_2 (e_s - e_a)}{\Delta + \gamma(1 + 0.34U_2)} \quad (3.8)$$

where; ET_o= reference evapotranspiration [mm day^{-1}], Rn= net radiation at the crop surface [MJ m^{-2}day^{-1}], G = soil heat flux density [MJ m^{-2}day^{-1}], T = mean daily air temperature at 2 m height [°C], U_2 = wind speed at 2 m height [ms^{-1}], es= saturation vapor pressure [kPa], ea= actual vapor pressure [kPa], Δ= slope vapor pressure curve [kPa °C^{-1}], γ = psychometric constant [kPa °C^{-1}].

3.3.5. Trend analysis

Trend analysis is important tool used in various fields. To identify patterns, forecasting and predicting for future values. Mann Kendall analysis was used to test consistency. Annual and seasonal data were corrected using this formula (Bekele et al., 2019).

$$Xi = f(ti) + \varepsilon i \tag{3.9}$$

Where, F (ti) is a continuous monotonic increasing or decreasing function of time and εi is assumed to be from the same distribution with zero mean.

$$S = \sum_{i=1}^{n-1} \sum_{j=1}^{n} sing[Tj - Ti] \tag{3.10}$$

where, Xi is annual values of years, J and i, j>i respectively

$$sing = \begin{cases} 1 \text{ if Tj} > \text{Ti} \\ 0 \; if \; Tj = Ti \\ -1 \; if \; Tj < Ti \end{cases} \tag{3.11}$$

$$Var(s) = \frac{1}{18}\left[n(n-1)(2n+5) - \sum_{p=1} tp(tp-1)(2tp+5)\right] \tag{3.12}$$

Where p is the number of tried groups and t_p is the number of data values in the P^{th} group. The values of S and Var(s) is to compute the test statistics Z. if ties are not occurred the variance can be calculated using Equation (3.13).

$$Var\ (s) = \frac{\text{n}(n-1)(2n+5)}{18} \tag{3.13}$$

Where, n is the number of tied grouping the time series data and t_i is denotes the number of ties up the number of sample i, when n is greater than 10, the standard normal z test statistics is calculated in Mann-Kendall as follows.

$$Z = \begin{cases} \frac{\text{s}-1}{\sqrt{\text{Var}(s)}}, If\ S > 0 \\ 0 \;\; If\ S = 0 \\ \frac{\text{S}+1}{\sqrt{\text{Var}(s)}}, If\ S < 0 \end{cases} \tag{3.14}$$

Z value is used to evaluate a statistically significant, a positive and negative values of z values indicates negative and positive upward and downward trend respectively.

3.3.6. Land use land cover classification and accuracy assessment

Accuracy assessment is the final step of classification process. The purpose of accuracy assessment is to quantitatively evaluate how pixels are effectively sampled in the correct of LULC classes. Kappa coefficient was used

$$\text{Kappa Coefficient (T)} = \frac{(TS*TCS)-\sum(Column\ total*Row\ total)}{\mathrm{TS}^2-\sum(Column\ total-Row\ Total)} * 100 \tag{3.15}$$

$$\text{Overall Accuracy} = \frac{Total\ Number\ of\ correctly\ classified\ Pixels(diagonal)}{Total\ Number\ of\ Reference\ Pixels} * 100 \tag{3.16}$$

3.4. Hydrological modeling

3.4.1. SWAT model performance evaluation

The accuracy, consistency, and adaptability of a model's performance must all be considered. A forecast efficiency criterion is also required to assess the model's performance. Nash Sutcliff (ENS) is a measure of the fit between the pattern of simulated and actual stream flows.

$$NSE = 1 - \frac{\sum_{i=1}^{N}\left(Q_{s,i} - Q_{o,i}\right)^2}{\sum_{i=1}^{N}\left(Q_{o,i} - \overline{Q}_o\right)^2} \tag{3.17}$$

Where; $Q_{s,i}$= simulated flow (m^3s^{-1}); $Q_{o,i}$= observed flow (m^3s^{-1}); $\bar{Q}_o$ =mean of observed flow (m^3s^{-1}).

R^2 (Coefficient of determination); it is the squared ratio between the covariance and the multiplied standard deviations of the observed and simulated values (Girma, 2012). It ranges between 0 and 1. A value of zero means no correlation whereas a value of 1 means strong correlation or that means the dispersion of the simulation is equal to that of the observation. It is calculated as;

$$R^2 = 1 - \frac{\sum_{i=1}^{N}\left(\left(Q_{s,i} - \overline{Q}_s\right)\left(Q_{o,i} - \overline{Q_o}\right)\right)^2}{\sum_{i=1}^{N}\left[\left(Q_{s,i} - \overline{Q}_s\right)\right]^2 \sum_{i=1}^{N}\left[\left(Q_{o,i} - \overline{Q}_o\right)\right]^2} \tag{3.18}$$

Where; $Q_{s,i}$= simulated flow (m^3s^{-1}), $\overline{Q}_s$ = mean of simulated flow (m^3s^{-1}), $Q_{o,i}$= observed flow (m^3s^{-1}), $\bar{Q}_o$ =mean of observed flow (m^3s^{-1}).

3.5.Accuracy of rainfall simulations from climate models

Statistical methods such as, PBias, RMSE, Correl and Coefficient of Variation (CV) are used in this study to evaluate the model simulation outputs of rainfall data.

Percent bias can be estimated

$$P_{BIAS} = \frac{\left(R_{RCM} - \overline{R}_{obs}\right)}{\overline{R_{RCM}}} x100 \tag{3.19}$$

Where, PBias= Bias; RRCM = Climate rainfall data over the catchment; $\bar{R}_{RCM}$ = Average rainfall data of the climate; $\bar{R}_{obs}$= Average observed rainfall data

The coefficient of variation (CV) can be estimated by

$$CV = \frac{\delta R}{\overline{R}} x100 \tag{3.20}$$

Where, CV= Coefficient of Variation; $\bar{R}$ = is average rainfall over the catchment; δ = indicates standard deviation

The Root Mean Square Error of a model prediction with respect to the estimated variable R_{RCM} is defined as the square root of the mean squared error:

$$RMSE = \sqrt{\frac{\sum_{i=1}^{N}\left(R_{RCM} - R_{obs}\right)^2}{N}} \tag{3.21}$$

Where, RMSE= Relative Mean Square Error; R_{RCM} = climate rainfall data over the catchment; Robs = Observed rainfall data over the catchment; N = Number of years that rainfall observed

Correlation Coefficient (Correl) can be estimated by using Equation (3.23).

$$correl = \frac{\sum_{i=1}^{n}\left(R_{obs} - \overline{R}_{obs}\right)\left(R_{RCM} - \overline{R}_{RCM}\right)}{\sqrt{\left(\sum_{i=1}^{n}\left(R_{obs} - \overline{R}_{obs}\right)^2 \sum_{i=1}^{n}\left(R_{RCM} - \overline{R}_{RCM}\right)^2\right)}} \tag{3.22}$$

R_{RCM}= Historical rainfall (mm), $\overline{R}_{RCM}$ = Mean of historical rainfall (mm), $R_{obs,}$= Observed rainfall (mm), $\bar{R}_{obs}$ = Mean of observed rainfall (mm).

3.6. Rainfall-runoff modeling using SWAT

SWAT applied the hydrological water balance which is the driving force for every hydrology study to analyze the essential characteristics of the watershed. The fundamental hydrology of a watershed in SWAT is based on the following water balance equation

$$SW_t = SW_o + \sum_{t=0}^{t} \left(R_{day} - Q_{surf} - E_a - W_{seep} - Q_{gw} \right) \tag{3.23}$$

Where; SW_t= final soil water content (mm water); *SW0* i = initial soil water content on day *i* (mm water), *t* is the time (days); *Rday*= amount of precipitation on day *i* (mm water); *Qsurf*= amount of surface runoff on day i (mm water); *Ea*= amount of evapotranspiration on day *I* (mm water), Wseep = amount of water entering the vadose zone from the soil profile on day *i* (mm water), and

Qgw= amount of return flow on day i (mm water).

Surface runoff occurs whenever the rate of water application to the ground surface exceeds the rate of infiltration. SWAT offers two methods for estimating surface runoff: the SCS curve number procedure and the Green &Ampt infiltration method as cited in (Neitsch et al., 2011).

$$Q = \frac{\left(R_{day} - I_a \right)^2}{\left(R_{day} - I_a + S \right)} \tag{3.24}$$

Where; Q = accumulated runoff or rainfall excess (mm H2O); R_{day} = rainfall depth for the day (mm H2O); I_a= initial abstractions which includes surface storage, interception and infiltration prior to runoff (mm H2O), and S is the retention parameter (mm H2O).

The retention parameter varies spatially due to changes in soils, land use, management and slope and temporally due to changes in soil water content. The retention parameter is defined as:

$$S = 25.4 \left(\frac{1000}{CN} - 10 \right) \tag{3.25}$$

Where; CN is the curve number for the day and it is a function of land use, soil permeability and antecedent soil water condition.

Commonly Ia is approximated by 0.2S and the above equation rewrite as follow: -

$$Q = \frac{\left(R_{day} - 0.2S\right)^2}{\left(R_{day} - 0.8S\right)} \quad (3.26)$$

SWAT calculates CN using soil classes and land uses classifications data.

The peak runoff rate is the maximum runoff flow rate that occurs with a given rainfall event. The peak runoff rate is an indicator of the erosive power of a storm and is used to predict sediment loss. SWAT calculates the peak runoff rate with a modified rational method.

$$Q_{peak} = \frac{\alpha_{tc} Qsur.Area}{3.6 t_{conc}} \quad (3.\ 27)$$

Where; $Qpeak$ = peak runoff rate (m^3s^{-1}); α_{tc}= fraction of daily rainfall that occurs during the time of concentration; Q_{sur} = surface runoff (mm), Area is the sub basin area (km^2), tconc is the time of concentration for the sub basin (hr) and 3.6 is a unit conversion factor. The general conceptual framework of this study is presented in Figure 3.8.

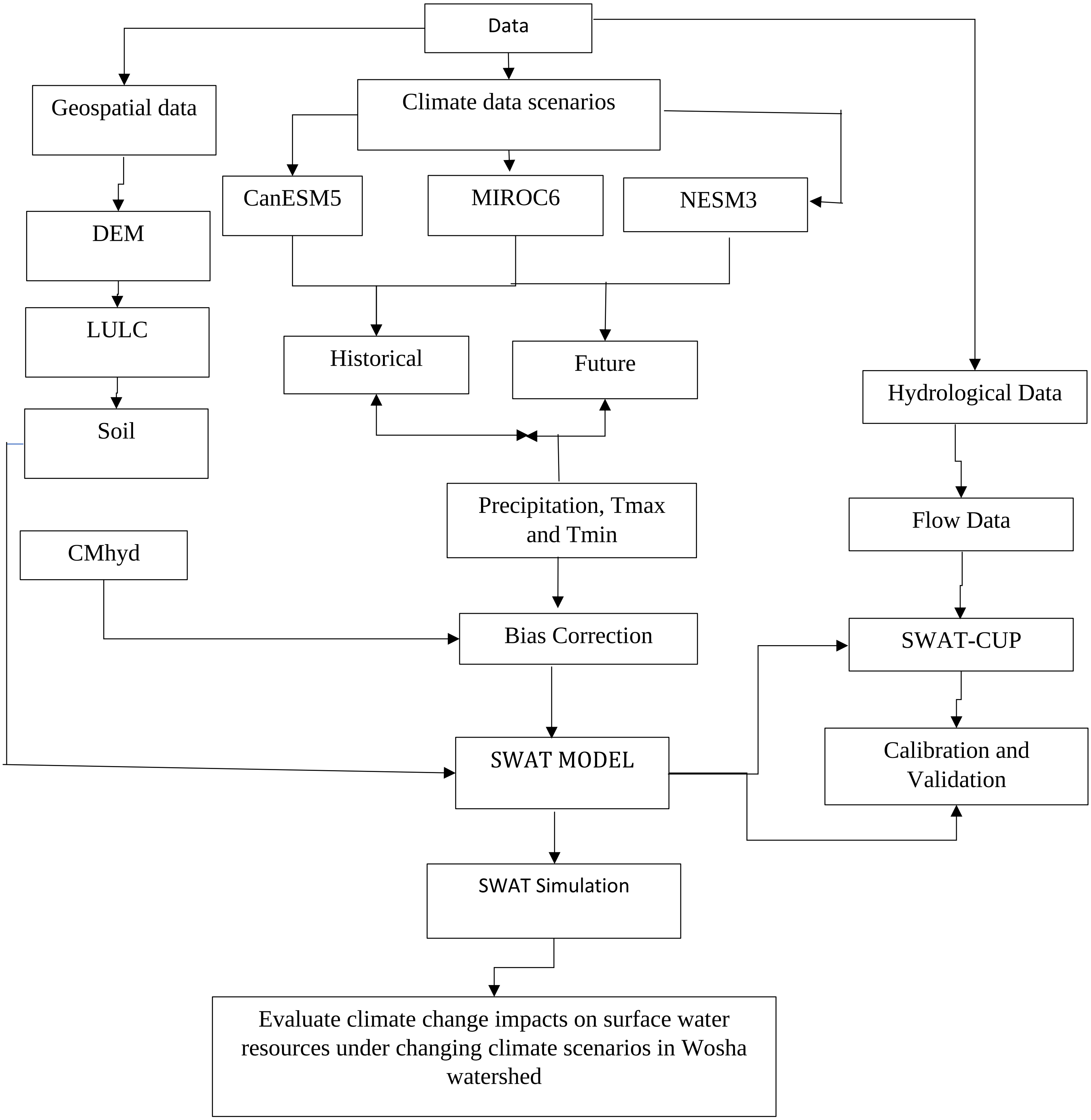
Data
Geospatial data
Climate data scenarios
DEM
CanESM5
MIROC6
NESM3
LULC
Historical
Future
Hydrological Data
Soil
Precipitation, Tmax and Tmin
Flow Data
CMhyd
Bias Correction
SWAT-CUP
SWAT MODEL
Calibration and Validation
SWAT Simulation
Evaluate climate change impacts on surface water resources under changing climate scenarios in Wosha watershed

Figure 3.8: Conceptual frame work of thesis

4. RESULTS AND DISCUSSION

4.1. Climate Change Scenario

The baseline climate scenario is a representation of the current state of the climate. This study used daily precipitation and temperature of observed data from 1988 to 2023. In the future scenario, the surface water availability was simulated, and stream flow was estimated using CanESM5, MIROC6, and NESM3 of CMIP6 models under SSP2-4.5 and SSP5-8.5 scenarios. The models were analyzed for three periods: the baseline period (1985-2014), mid-term forecasts 2050s or (2041-2070), and long-term projections 2080s or (2071-2100). For comparison, a baseline period covering the years 1985 to 2014 was employed. Temperature (Tmax and Tmin) and precipitation have been forecasted for the mid-term (2041–2070) and long-term (2071–2100) periods.

4.1.1. Uncorrected Rainfall and Temperature Analysis

Rainfall and temperature projections have been frequently derived from hydrological models powered by the Global Climate Models (GCMs) in recent years. The watershed's observed rainfall was overestimated, underestimated, and overlayed to the simulation rainfall (Figure. 4.1). The MIROC6 model underestimated observed rainfall for November and December. The model CanESM5 was overestimated in November. The model NESM3 was underestimated in February to April, and overestimated in November and December.

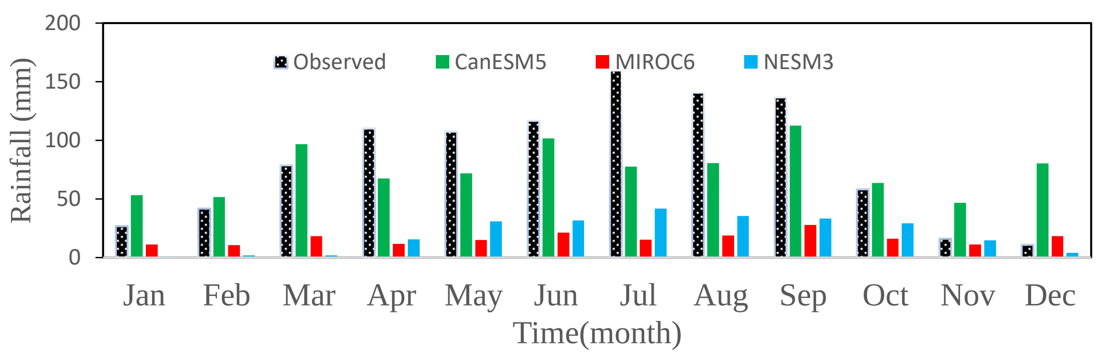

Figure 4.1: Baseline monthly uncorrected rainfall (1985–2014)

The watershed's observed maximum temperature was overestimated and understated by the climate models (Figure 4.2). The measured maximum temperature was slightly overestimated by

CanESM5 in March. MIROC6 and NESM3 were underestimated in all months. Also, the model CanESM5 was underestimated in all months except for March. The observed minimum temperature of the watershed was underestimated and slightly overlayed by the climate models except the model NESM3 in the January, November, and December months underestimated (Figure 4.3).

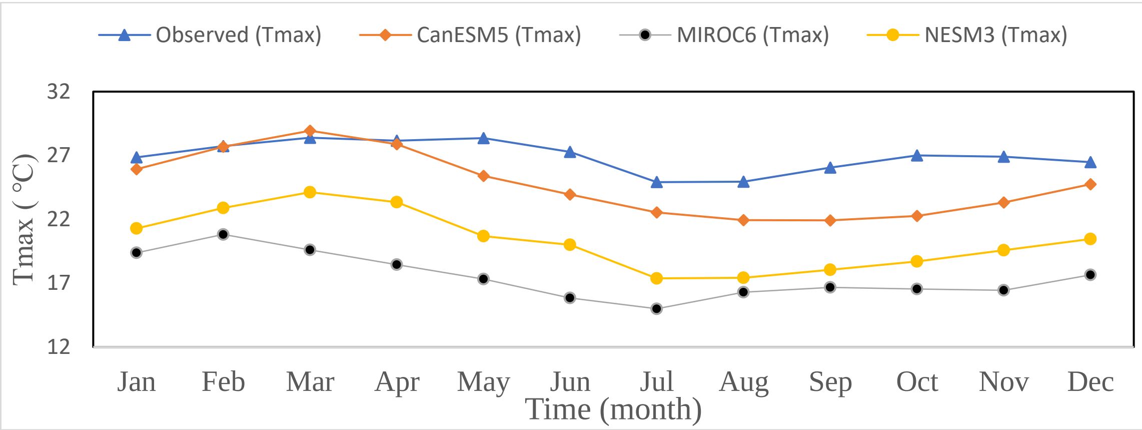

Figure 4.2: Baseline monthly uncorrected maximum temperature (1985–2014).

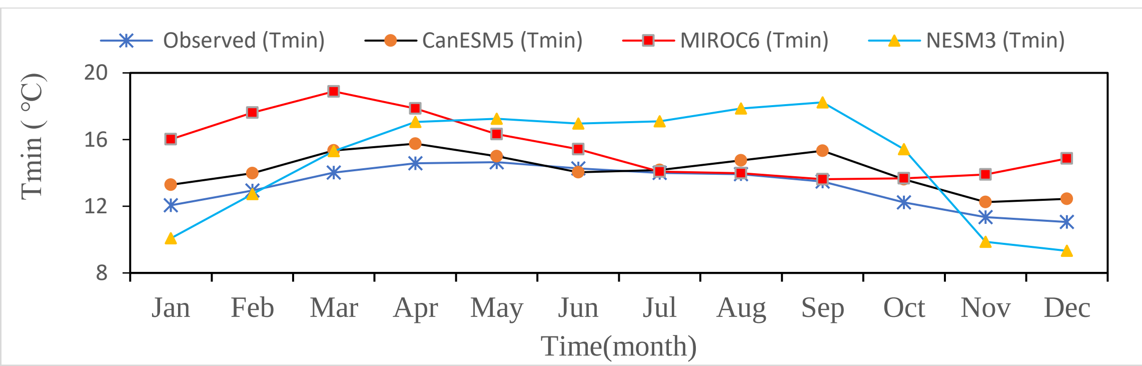

Figure 4.3: Baseline monthly uncorrected minimum temperature (1985–2014).

4.1.2. Performance Analysis of Climate Models

Climate models in hydrology modeling involve evaluating the accuracy of the models in simulating hydrological processes such as precipitation, temperature, runoff, and stream flow. This analysis typically includes comparing model outputs with observed data to assess the model's ability to capture the spatiotemporal variability of hydrological processes. The results of the performance analysis can be discussed in terms of various metrics such as statistical measures (e.g., correlation coefficient, Nash-Sutcliffe efficiency), graphical comparisons (hydrographs, scatter plots), and spatial patterns (spatial distribution of simulated vs. observed variables). The

Wosha watershed's yearly average rainfall predicted by climate models was compared. Table 4.1 shows the watershed's simulated and observed yearly average rainfall. A negative bias indicates that the model underestimates the rainfall compared to observations, while a positive bias indicates an overestimation. For example, CanESM5 has a bias of -2.62%, meaning it underestimates the rainfall by 2.62% compared to the observed data. The CV % represents the variability of the data relative to its mean. A higher CV % indicates higher variability. MIROC6 has the highest CV % at 30.88%, suggesting that its annual average rainfall data has higher variability compared to the other models. The RMSE represents the square root of the average of the squared differences between model predictions and observed values. A lower RMSE indicates better model performance in replicating the observed data. In this case, NESM3 has the lowest RMSE at 203.68 mm/year, indicating that it is closest to the observed data in terms of rainfall prediction accuracy.

The strength and direction of a linear link between two variables are determined by the correlation coefficient. A correlation value closer to 1 or -1 indicates a strong positive or negative relationship, respectively. MIROC6 has a high positive correlation of 0.69, suggesting a strong positive linear relationship between its predicted rainfall and observed data. In summary, when discussing the annual average rainfall data for each model: CanESM5 underestimates rainfall with a moderate bias and low correlation. MIROC shows higher variability but a strong positive correlation with observed data. NESM3 has the lowest RMSE, indicating better accuracy in predicting annual average rainfall compared to other models. The accuracy of simulated and observed rainfalls varies. CanESM5 has the lowest bias (-2.62%), indicating higher performance, while NESM3 has the highest value (2.58%). The model performed better in terms of (Corr = 0.69). There is less fluctuation between the observed and simulated rainfall, as evidenced by the CV value of NESM3 (11.58%), which is near the observed value (11.15%). The CanESM5 (1097.9 mm/year) model attempted to replicate the 1333.5 mm/year average yearly rainfall that was recorded.

Table 4.1: Rainfall's annual cycle performance.

Observed and GCM-RCM	Annual average rainfall (mm/year)	Bias (%)	CV (%)	RMSE (mm/ year)	Corr (-)
Observed	1333.5	---	11.15		---
CanESM5	1097.9	-2.62	27.36	209.18	-0.07
MIROC	1011.8	1.62	30.88	213.87	0.69

NESM3	1059.7	2.58	11.58	203.68	0.51

The performance of the climate model in capturing the highest temperature is shown in Table 4.2. It demonstrates that the ensemble mean (corr = 0.49) has outperformed the other models run by the CanESM5 model. However, the NESM3 model did not perform well in terms of CV (CV = 0.87%) and bias (bias = 9.12%).

Table 4.2: Performance of the climate model in capturing the maximum temperature (yearly statistics) from 1985 to 2014

Observed and climate models	Average annual Tmax (°C)	RMSE (°C)	Corr (–)	Bias (%)	CV (%)
Observed	25.6	1.20	-	-	-
CanESM5	24.5	1.49	-0.05	-5.02	1.43
MIROC6	23.4	1.41	0.31	- 4.98	0.67
NESM3	25.3	2.32	0.39	9.12	0.87
Ensemble mean	24.7	0.81	0.49	-1.89	0.5

Table 4.3 displays the results of the simulated average lowest temperature. The performance of the CanESM5 and MIROC6 models was good (corr = 0.52). Out of all the models, the NESM3 model displayed the least bias (bias = 43.12%). In terms of RMSE, the MIROC6 model did the poorest (RMSE = 12.02 °C). The observed minimum temperature was overestimated by all climate models. The performance evaluation criterion verified the minimum temperature and the ensemble mean ultimately satisfied the criteria.

Table 4.3: Accuracy of annual minimum temperature (1985–2014)

Observed and climate models	Average annual Tmin (°C)	RMSE (°C)	Corr (–)	Bias (%)	CV (%)
Observed	13.1	-	-	-	14.11
CanESM5	18.9	11.12	-0.03	35.80	13.89
MIROC6	20.8	12.02	0.32	41.98	15.22
NESM3	22.3	13.11	0.39	43.12	8.94
Ensemble mean	10.98	9.22	0.52	14.97	13.13

4.1.3. Bias-Corrected Climate Model

The large systematic errors in the climate model simulations were corrected with the bias adjustment. After bias correction, the observed rainfall was caught in the model CanESM5, MIROC6, and NESM3 (Figure 4.4). Therefore, bias-corrected climate model output should come before hydrological modeling. Following bias adjustment, the observed maximum, and minimum temperatures were recorded by the model CanESM5, MIROC6, and NESM3. Now that the observed and simulated data were identical following systematic error reduction, we may utilize the model output with confidence in the rainfall-runoff modeling of the watershed. Trends in the observed minimum temperature were captured by the models' bias-corrected minimum temperatures (Figure 4.5).

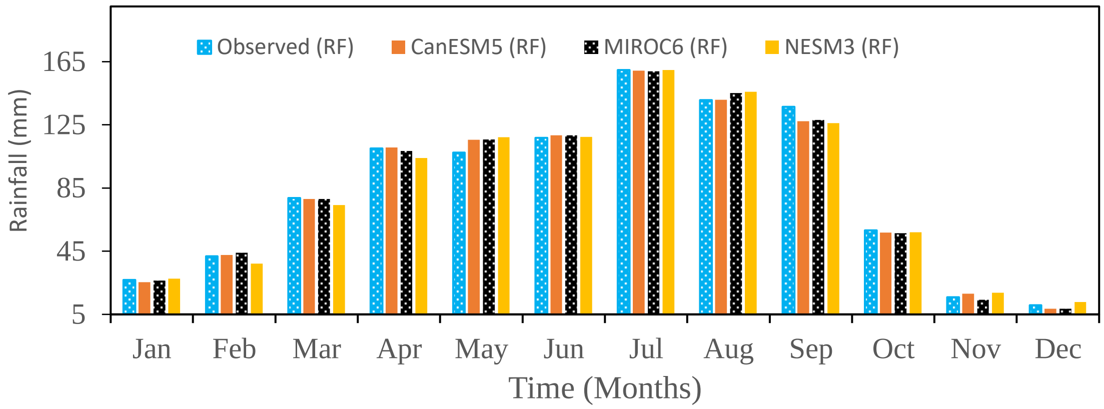

Figure 4.4: Monthly bias-corrected rainfall (1985–2014)

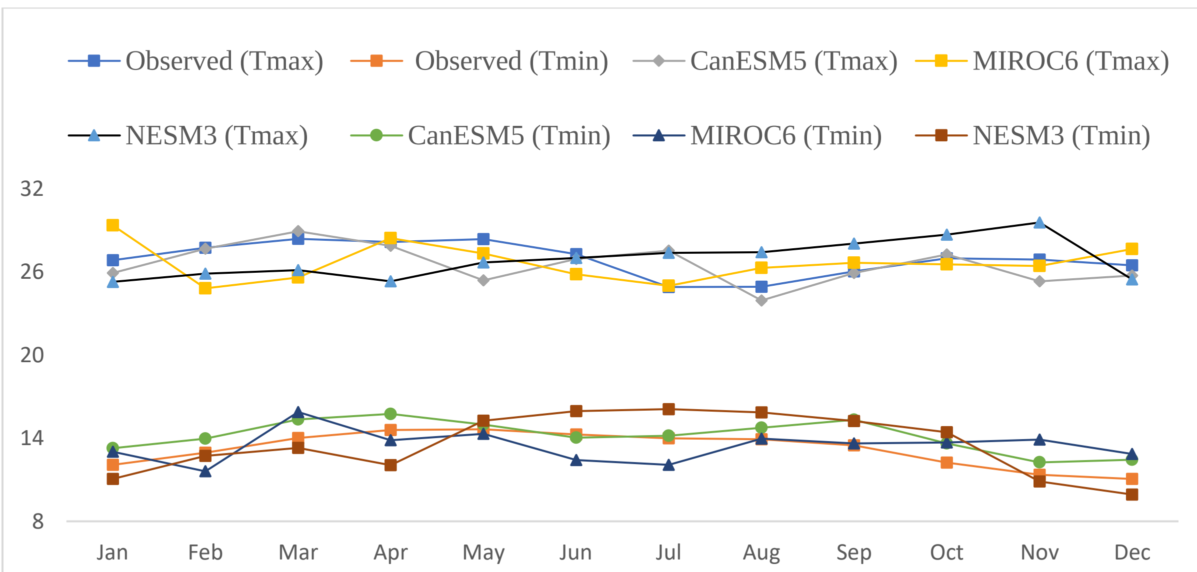

Figure 4.5: Monthly bias-corrected max. and min. Temperature (1985–2014)

4.1.4. Assessment of climate models performance

The climate model simulations underestimated and overestimated the observed annual rainfall (Table 4.4). Accuracy of dynamically downscaled rainfall from three climate models over overlapping period (i, e., observed rainfall and historical rainfall of the watershed) (1987–2005) is shown in Table 4.4.

Table 4.4:Downscaled rainfall from three climate models historical and observed

	Annual rainfall (mm)	Bias (%)	CV (%)	RMSE (mmyear-1)	Correlation Coefficient (-)
Observed	1391.83	-	16.8	-	-
CANESM5	1136.78	-0.46	25.38	8.49	0.16
MIROC6	1099.16	-8.86	73.94	2.77	0.21
NESM3	1219.14	0.23	24.34	8.78	0.46
Ensemble mean	1151.69	-3.03	20.14	2.46	0.49

4.2. SWAT model inputs analyzed and discussed

SWAT requires daily or sub-daily meteorological data and the model can either read these meteorological data from previously measured data stored in tables or can be arranged using a pcpSTAT and Dew02 model. The climate data is among the most prerequisite parameter of SWAT model, those are daily rainfall, maximum and minimum temperature, wind speed, relative humidity, solar radiation and arranged on a daily basis.

4.2.1. Digital elevations model

DEM well define the topography of the area by describing the elevation of any point at a given location and specific spatial resolution as a digital file. It is one of essential spatial input for SWAT to delineate the watershed in to a number of sub watersheds or sub basins based on elevation. Drainage pattern, slope, channel width and stream length with in the watershed were processed using DEM. Figure 4.6 shows DEM of Wosha watershed.

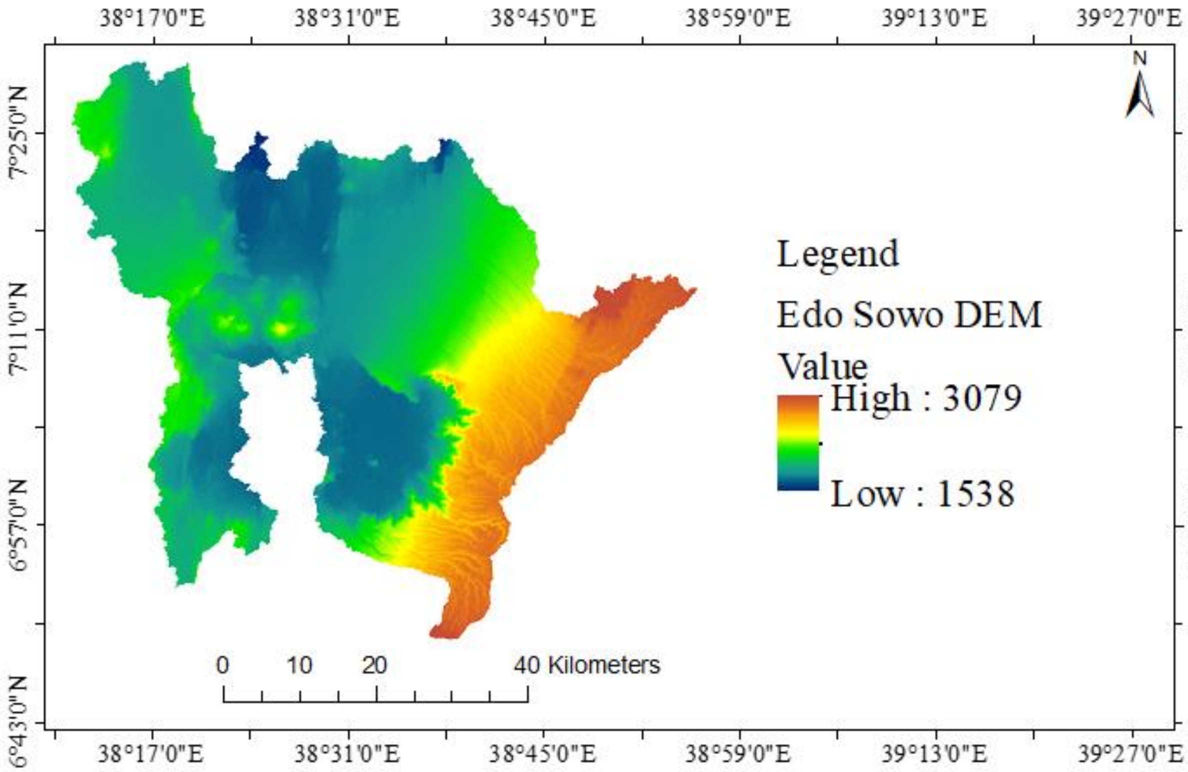

Figure 4.6: Wosha watershed Digital Elevation Model (DEM) used for SWAT model development

4.2.2. Soil data

Soil, land use and rainfall are the major physical watershed characteristic that governs runoff generation. The infiltration capacity of the soil depends on the porosity of the soil, which determines its storage capacity and affects the resistance of the water to flow into deep layers. Since the soil infiltration capacity depends on the soil texture, the highest infiltration rates are observed in sandy soil.

SWAT model requires different soil textural and physio-chemical properties, soil texture, available water content, hydraulic conductivity, bulk density, and organic carbon content for different layers of each soil type. The major soil groups of the Wosha watershed as per FAO soil groups found in the study area were Dystric Nitisols, Pellic Vertisols, Chromic Luvisols, Vitric Andosols, Leptosols, Eutric Nitisols, Eutric Fluvisols, Eutric Rapticsols and Orthic Acrisols (Table 4.5 and Figure 4.7).

Table 4.5: Major soil types and their area coverage in the Wosha watershed

Soil types	Area in (km^2)	Area in (%)	SWAT code
Pellic Vertisols	265.01	9.30	Pellicv
Eutric Fluvisols	127.01	4.46	Eutricf
Leptosols	1400.25	49.2	Leptosol
Chromic Vertisols	371.01	13.01	Chromiv
Chromic Luvisols	335.57	11.8	Chromicl
Orthic Acrisols	116.8	4.1	Orthics
Dystric Nitisols	30.28	1.06	Dystricn
Vitric Andosols	20.53	0.72	Vitrica
Eutric Nitisols	18.07	0.63	Eutricn
Eutric Rapticsols	110.78	4.13	Eutricr
Calcic Chernozem	41.01	1.44	calcicx
Luvic Phaeozem	12.05	0.42	luvicph
Total	2848.31	100	

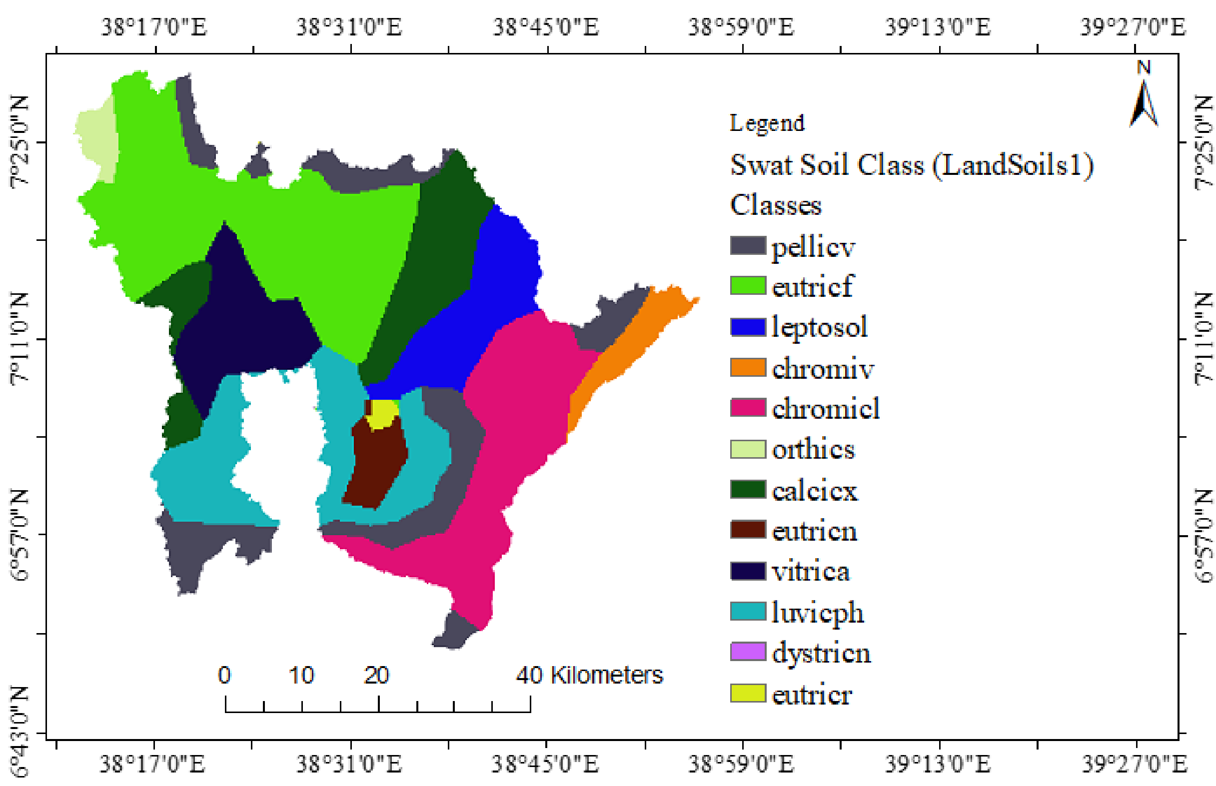

Figure 4.7: SWAT soil classes used in analysis and development in Wosha watershed

4.2.3. Land use/Land cover used for SWAT development

LULC it is spatial data set in the model defines the densities and types of land use found within a given area. Land use is one of the most important factors that affect runoff, Evapotranspiration and surface runoff in a watershed. Land use land cover data which is very essential for SWAT input for determining the watershed characteristics, and also used for comparison of impacts on runoff and sediment yield of the watershed.

Land cover and soil are factors greatly influencing the hydrological properties of a watershed that are required by SWAT to describe a sub-basin or HRU. Once watershed topographic parameters have been computed for each sub basin, the interface uses land cover and soils data to generate multiple hydrologic response units (HRUs) within each sub basin by GIS overlay process to assign soil parameters and SCS curve numbers. HRUs were lumped land areas within the sub watershed that are comprised of distinctive land cover, soil, and management combinations (Neitsch et al., 2002). Such subdivision of sub-basins in to HRUs enables the SWAT model to reflect the spatial variations of the hydrologic conditions for different land cover and soil distributions within the sub-basins.

Land use and land cover of the Wosha watershed was downloaded from USGS website as shown in Table 4.6 and Figure 4.8. The data contain the redefined land use of the area. In the land use attribute table integer values interred for the same land covers.

Table 4.6: Major Land Use/Land Cover and their area coverage in the Wosha watershed

Major land use land cover	Area in (Km2)	Area in (%)	SWAT code
Agricultural Land-Generic	354.57	12.44979	AGRL
Agricultural Land-Row Crops	7.54	0.264747	AGRR
Shrubland; Dense (>50% woody cover)	52.87	1.85639	RNGB
Water	51.19	1.797402	WATR
Summer Pasture	14.5	0.509129	SPAS
Urban Agriculture	1240	43.53933	URBN
Range-Grasses	375	13.16713	RNGE
Forest-Mixed	354	12.42978	FRST
Wetlands-non-forested	274	9.620787	WETN
Pasture	124.5	4.371489	PAST
Total	2848.17	100.006	

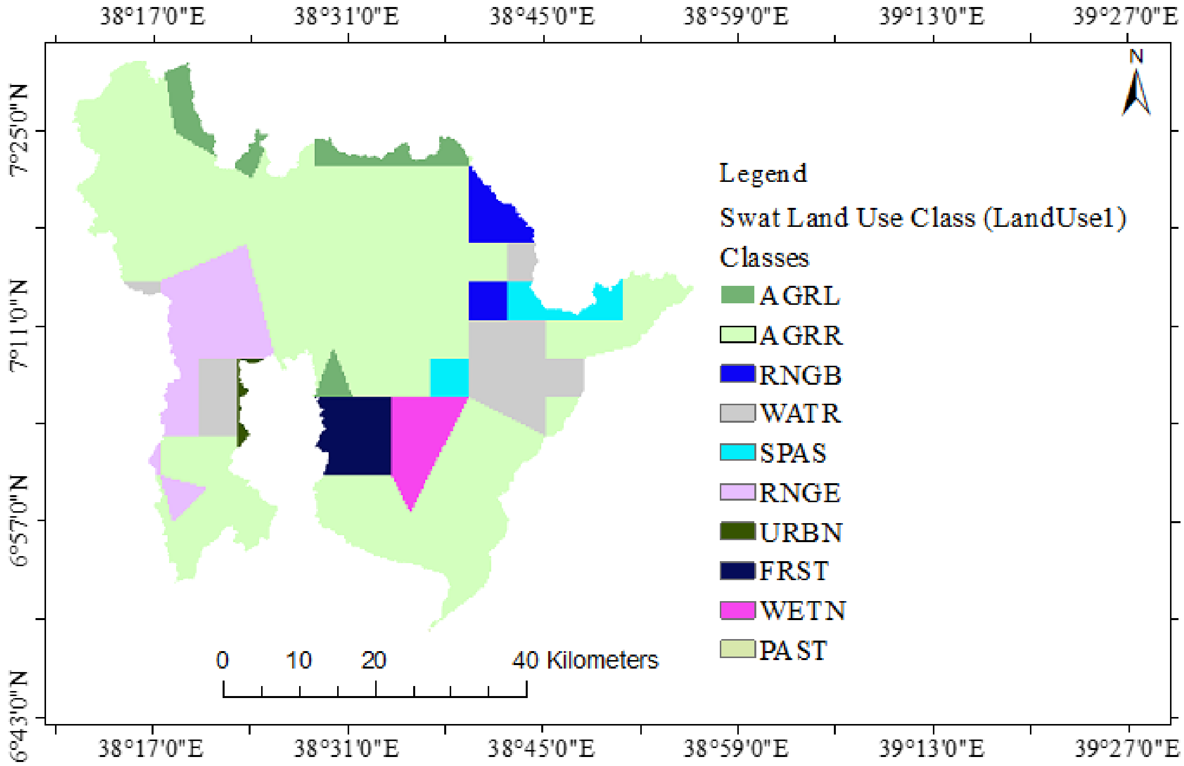

Figure 4.8: Land use land cover used for SWAT development in Wosha watershed

4.2.4. Data preparation and sub-basin discretization for SWAT model developed

The required spatial data sets were projected to the same projection called Adindan UTM Zone 37, which is the transverse Mercator projection parameter for Ethiopia, using Arc GIS 10.7 The land use / Land cover special data were decalcified in to SWAT land cover/plant types. A user lookup table was created that identified the SWAT code for different categories of Land cover/Land use on the map as per the required format. The soil map is linked with the soil data base which is designed to hold data for soils not included in the U.S.

4.2.5. Watershed delineation

The watershed and sub watershed delineation were done using DEM data. The watershed delineation process includes some major steps such as, DEM setup, stream delineation, outlet and inlet definition, watershed outlet selection and definition and calculation of sub basin parameters. For the stream definitions the threshold-based stream definition option was used to define the minimum size of the sub basins. The Arc SWAT interface allows the user to fix the number of sub basins by deciding the initial threshold area. The threshold area defines the minimum drainage area required to form the origin of a stream. Sub dividing the sub watershed in to areas having unique land use, soil and slope combinations makes it possible to study the differences in evapotranspiration and other hydrological conditions for different land covers, soil and slopes. The land use, soil and slope data sets were imported, overlaid and linked with SWAT 2017 data base.

The monitoring points are added manually and the numbers of sub basin were adjusted accordingly. Finally, the watersheds were delineated and its area of 2848 km^2 and 73 sub basins were generated for the watershed as shown on Figure 4.9.

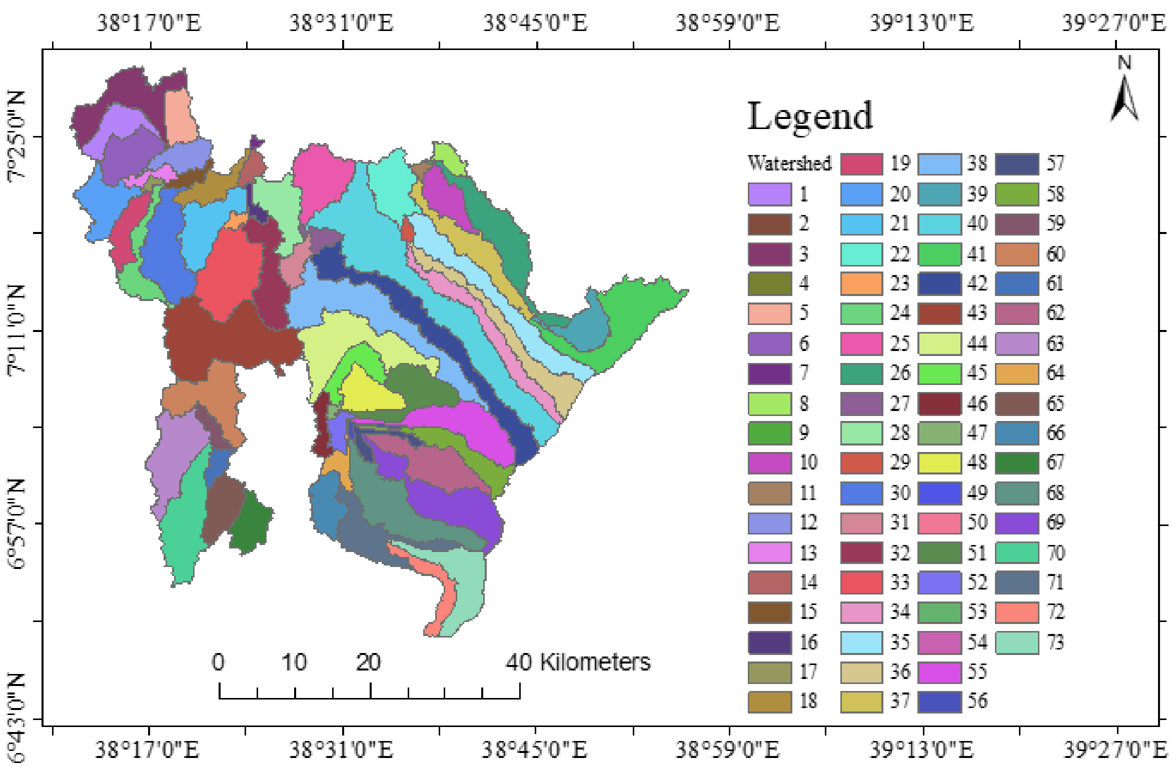

Figure 4.9: Wosha sub basins used in SWAT model development and model simulations

4.2.6. Hydrologic response unit (HRU) definition

After watershed delineation, the watershed was partitioned into a hydrological response unit. The Hydrologic Response Units (HRUs), are combinations of land use, soil, and slope within the watershed. The HRU analysis tool in Arc SWAT helps to load land use, soil layers, and slope maps to the project. The delineated watershed by Arc SWAT and the prepared land use and soil layers were overlapped 100%. Process based on a certain threshold values of soil/land use combinations.

In this study multiple HRUs was selected. The soil and land use classes in the input soil and land use map were decoded using a lookup table, a table created by the user in txt format according to SWAT input file format. Table 4.4 shows lookup table of land use and soil type of the study area. There for four classes of land use and soil map was renamed into twelve classes of SWAT database as shown in the (Figure 4.7 and Figure 4.4).

Table 4.7: Lookup table of land use and Soil type

Value	Land Use	Value	Soil Class
24	AGRL	1	Pellicv
18	AGRR	2	Eutricf
131	RNGB	3	Leptosol
142	WATR	4	Chromiv
155	SPAS	5	Chromicl
160	URBN	6	Orthics
162	RNGE	8	Eutricn
167	FRST	9	Vitrica
170	WETN	11	Dystricn
178	PAST	12	Eutricr

HRU analysis in SWAT includes divisions of HRUs by slope classes in addition to land use and soils. The multiple slope option was selected for this study. In this particular study, the slope of the watershed was discretized in to recommended slope classes as shown in Figure 4.10. The slope of the watershed was necessary spatial data required by SWAT model integrated with Hydrologic Response Unit.

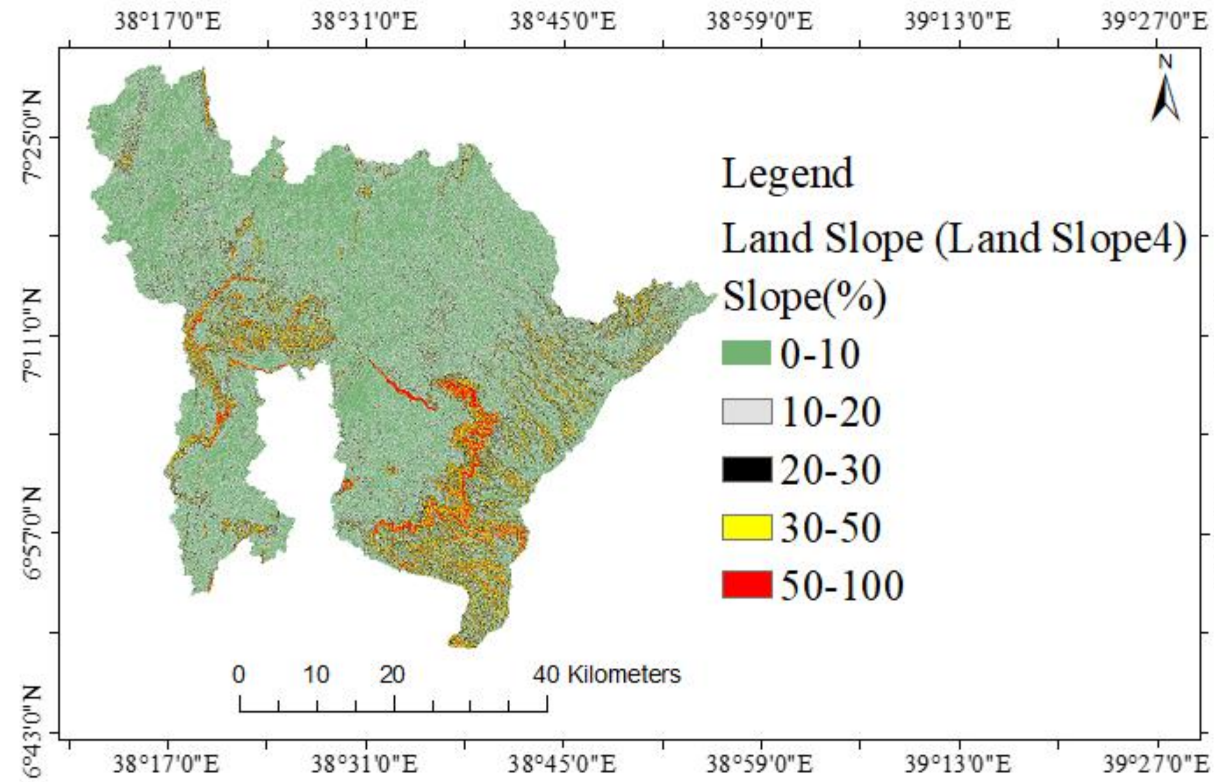

Figure 4.10: Slope classes of Wosha watershed

The HRU analysis section takes land use, soil and slope data, and divides each sub basin in to HRU with specific combinations of the three-layer respective characterization. The layer produced by this process is crucial to the ultimate analysis performed by the SWAT model, because it determines the land use, soil and slope category assigned to each HRU. This category determines how land will respond to precipitation, run off, infiltration and other hydrologic processes during the simulation. Each sub basin can then have one or more major HRUs defined within it. Finally total of 157 HRUs for 73 sub basins were created (Figure 4.11). And then subdividing the sub watershed into areas having unique land use land cover, soil and slope combinations makes it possible to study the differences in evapotranspiration and other hydrologic conditions for different land covers, soils and slopes.

The land use, soil and slope datasets were imported overlaid and linked with the SWAT 2017 databases. To define the distributions of HRUs multiple HRU definition options were tested. For multiple HRU definition 20 percent land use, a 10 percent soil and 10 percent slope threshold were used as an adequate for most applications. After fulfilling the entire above requirement obtain full HRU map of the watershed as indicated below.

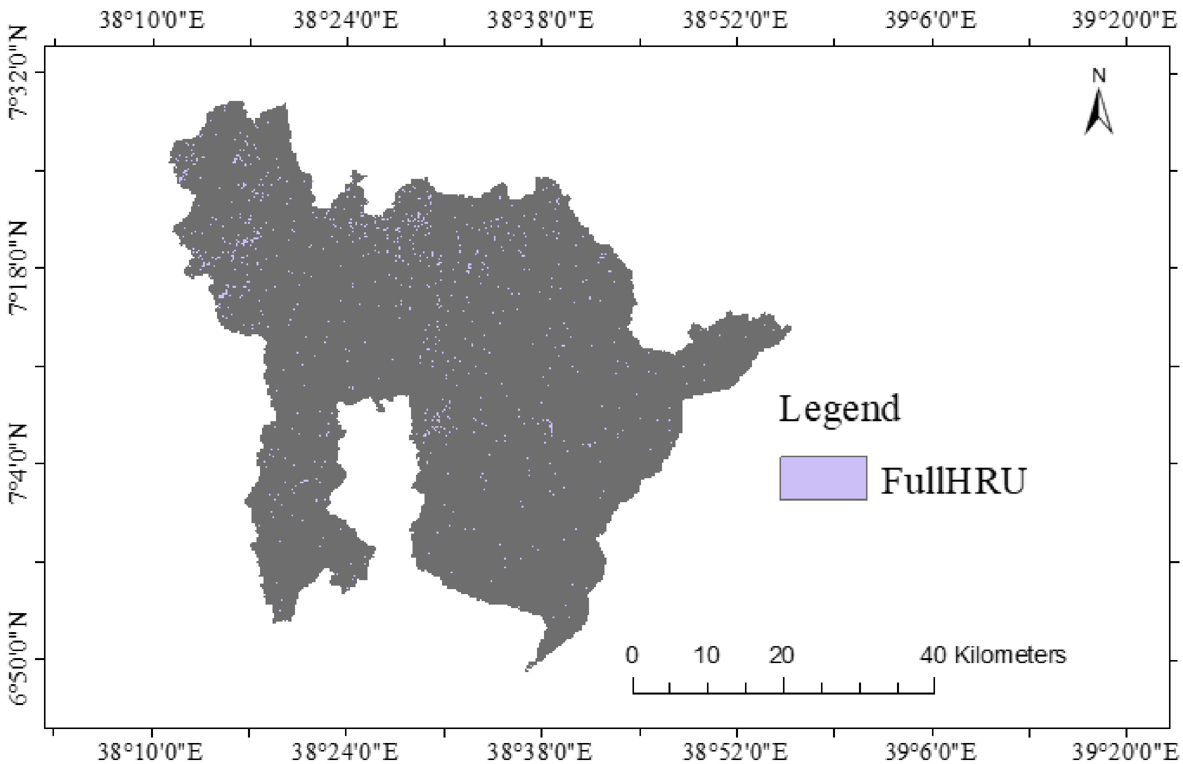

Figure 4.11: Full hydrologic response unit (HRU) of Wosha watershed

4.3. SWAT model sensitivity analysis, calibration and validation

After all the required inputs for the model were analyzed and prepared according to the model format, the watershed delineation was conducted from 30 by 30 DEM resolution and the model delineates an area of 2848 km^2, provided that the outlet location is at lowest point of the river. The land use/land cover, soil and slope map of Wosha watershed was overlay to produce a hydrologic response group by setting a thresh hold value of 5, 20 and 20% for land use/land cover, soil and slope respectively.. The land use, soil and slope

domination to which land use percentage over the sub basin, soil over the land use and slope class percentage over the land use respectively selected by considering the effect of on the formulation of hydrologic response in the final water balance results and for making the HRU formulation in a manageable amount. Accordingly, 73 sub basins having 157 HRUs created in the watershed.

4.3.1. SWAT model sensitivity analysis

Sensitivity analysis was carried out before calibrating the model to save time during calibration. In this study, identifying sensitive parameters enables to focus only on those parameters which affect most the model output during calibration since SWAT model has a number of parameters to deal with. Some parameters do not have any influence on the model output while some may have little effect.

4.3.2. Parameters sensitive to streamflow

Water availability assessments were done by soil and water assessment tool (SWAT) hydrological model with different sensitivity parameters. Even though there were more than 26 sensitivity parameters those were used for flow calibration, around 11 parameters were selected for this study. Those 11 parameters are sensitive, were used to calculate the amount of runoff from the watershed. The parameter identification was done by using the monthly flow data from 1987 to 2006.

According to the result from the global sensitivity analysis, base flow recession constant (ALPHA_BF) was found to be the most sensitive parameter followed by available water capacity (mm water/mm soil) (SOL_AWC), initial Soil Conservation Service (SCS) runoff curve number for moisture condition II (CN2), Deep aquifer percolation fraction (RCHRG_DP) and Average slope length (SLSUBBASIN) ranking up to fifth position. Based on the analysis result, Average slope steepness (HRU SLP), Groundwater "revap" coefficient (GW_REVAP), Soil evaporation compensation factor (ESCO) was relatively less sensitive parameters in runoff simulation. On the other hand, parameters such as Depth from soil surface to bottom of layer (SOL_Z), threshold depth of water in the shallow aquifer required for return flow to occur (GWQMN) were found to be least sensitive in flow simulation.

4.4. Flow calibration and validation

4.4.1. Flow calibration

Most models are provided with default values of the parameters. However, in this case initial values of the model parameters were defined. The minimum and maximum acceptable values were provided based on the information of related pervious works and literatures (Ayele et al., 2022). The best parameters obtained were compared to the predicted flows. Then SWAT_CUP calibration was run for the periods of the hydrological year 2001-2010 while 2011-2015 for flow validation and 2001 and 2002 for model warm-up. The calibrated and validated values of the parameters were used in the iteration of calibration and validation (Table 4.8). The calibrated and validated parameters are within the range of the suggested values of SWAT.

The calibration and validated result indicate good agreement between monthly measured and simulated flows Figure 4.12. The scatters plot of the values of the measured and the simulated monthly stream flows data has also shown a fair linear correlation between the two data sets. The trend and the magnitude of the two data set values are shown in Figure 4.12 and Figure 4.13 for calibration and validation respectively.

Table 4.8: Summary of calibrated flow parameters

Parameter	Rank	SWAT-CUP range	Fitted Values
RCHRG_DP	1	0-1	0.86018
CN2	2	-0.25-0.25	0.118
SLSUBBSN	3	-0.5	0.249112
SOL_Z	4	-0.5	0.2396
Gw-Delay	5	0-500	438.18
GW_REVAP	6	0.02-0.2	0.1933
ALPHA_BF	7	0-1	0.9268
HRU_SLP	8	-0.5	0.056
SOL_AWC	9	-0.5	0.223
GWQMN	10	0-5000	498.34

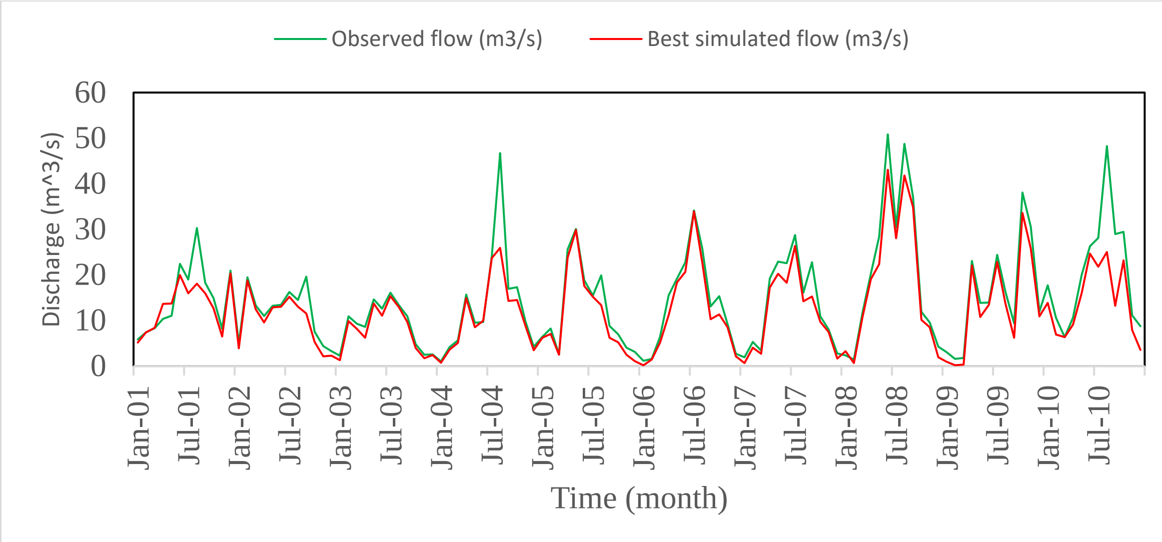

Figure 4.12: Comparison of observed monthly flow with a simulated (calibrated) monthly flow of Wosha watershed at the outlet (2001-2010).

The calibration and validation results in Table 4.9 show that there is a good agreement between the simulated and gauged monthly flows. This is demonstrated by the goodness-of-fit measures correlation coefficient (R^2 = 0.77), and the Nash-Sutcliffe Simulation efficiency (NSE=0.75). The result fulfilled the requirement suggested by (Santhi et al., 2001).

Table 4.9: Calibration and validation statistics of average monthly simulated and gauged flows at the outlet of Wosha watershed.

Objective function	Calibration (2001-2010)	Validation (2011-2015)
NSE	0.75	0.72
R^2	0.77	0.80

4.4.2. Flow validation

As it is mentioned above the purpose of model validation is to establish whether the model has an ability to estimate output hydrology for other time periods or conditions than those for which the parameter values were adjusted to fit. Model validation involves re-running the model using input data independent of data used in calibration (e.g., differing time period), but keeping the calibrated parameters unchanged. In this case, flow data from a period from January 1, 2001 to December 31, 2006 at outlet of Wosha watershed were used to validate the model for a monthly time-period.

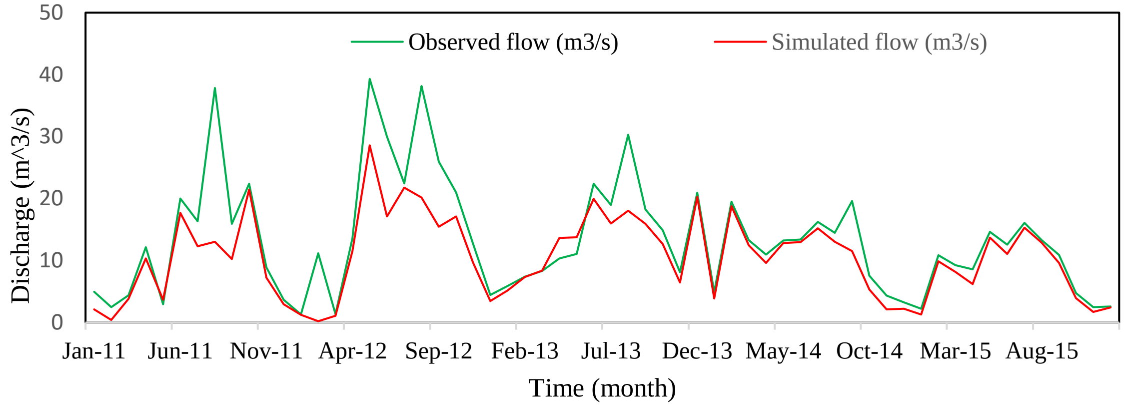

Figure 4.13: Comparison of observed monthly flow with a validated monthly flow of Wosha watershed (2011-2015).

A good agreement between monthly observed and simulated flows at the outlet of the watershed during validation processes is shown in Table 4.9 and the goodness-of-fit measures the coefficient of correlation (R^2 =0.83), and Nash-Sutcliffe simulation efficiency (NSE=0.72).

Generally, this validation/calibration check illustrates the accuracy of the model for simulating periods outside of the calibration period. Since the model performed as well in the validation period of 2011-2015, as for the calibration period of 2001-2010 at the outlet of Wosha as indicated in the above Tables 4.6 and Figures 4.9 hence the set of sensitive parameters listed in Table 4.3 during calibration process for the watershed can be taken as the representative set of parameters for the Wosha watershed.

4.5. Assessment of the spatial and temporal distribution of rainfall and discharge in Wosha watershed

Trend analysis is used to detect long-term changes in the pattern of precipitation and temperature in this watershed. Such changes in the pattern of precipitation and temperature over a region are the most important indicators of climate change. Trend analysis is used to understand where and to what extent climate is changing. Streamflow trends provide valuable information for water resources management. Predicting changes in streamflow can assist in future water management plans as well as responses to drought or flood conditions. Mann-Kendall trends show the highest peak occurs 2015 reaching above 700mm. There are other noticeable peaks 1997 and 2019 could be considered as an outlier as it is very different from the other values.

4.5.1. The Baseline Period's Rainfall and Temperature Variability (1985–2014)

From January to March, the entire climate model showed an increasing sign. However, from September to December, the models displayed a decline (Figure 4.6). The lowest rainfall (8.56 to 15.32 mm/month) was recorded by the MIROC6 models in November and December, respectively. From October to December, all climate models simulated monthly rainfall declined marginally. In August, high rainfall was recorded by the CanESM5 and MIROC6 models (184.11 and 183.79 mm/month, respectively) (Figure 4.14).

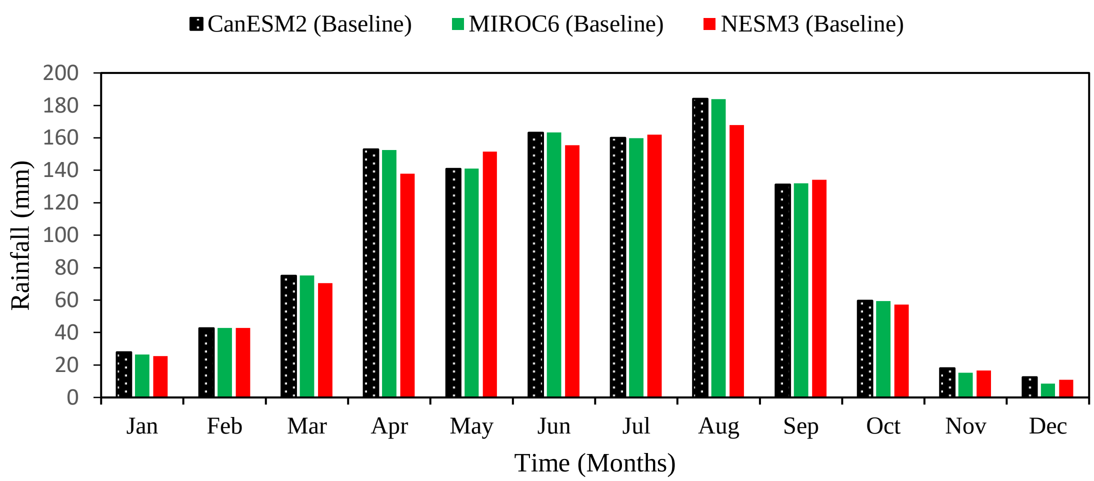

Figure 4.14: Baseline monthly rainfall change (1985–2014).

The monthly maximum and minimum temperatures showed an increasing trend across all climate models from January to March and from September to December (Figure 4.15). However, the models indicated a decline from April to August. In March and November, respectively, the monthly maximum temperature (28.82°c ± 1.5°c and 28.38°c ± 1.5°c) was recorded by the NESM3 models. In March, the MIROC6 model recorded 27.33°c ±1.5°c, while the CanESM5 models recorded a high maximum temperature of 28.26°c ± 1.5°c (Figure 4.15).

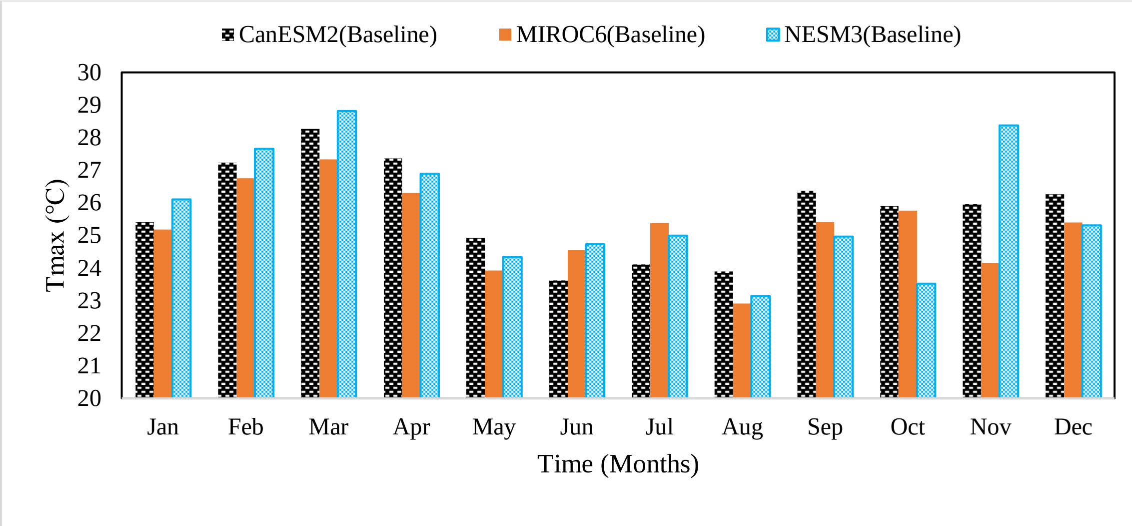

Figure 4.15: Baseline Maximum Temperature Change (1985–2014)

In August, the minimum temperature predicted by all climate models for the Wosha watershed was a low 9.9°C ± 0.5°C (Figure 4.16). Conversely, the MIROC6 model indicated a high minimum temperature of 16.35°c ± 0.92°c for November, and also, the high minimum temperature for March was 14.97°c ± 2.1°c recorded for the CanESM5 model (Figure 4.16).

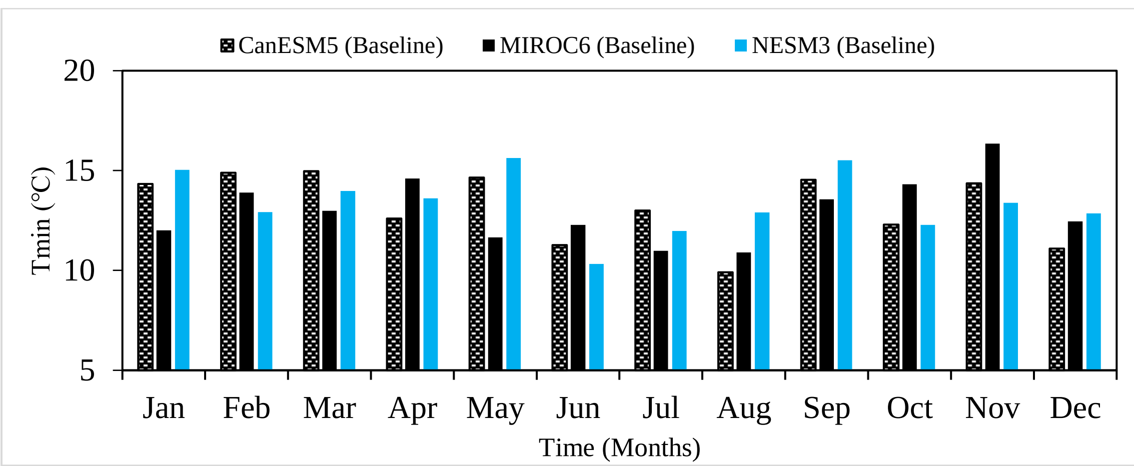

Figure 4.16 Baseline Minimum Temperature Change (1985–2014)

4.5.2. Projected Variation in Temperature and Rainfall in Mid-Term Scenarios.

The simulation of monthly rainfall in the mid-term periods by the climate models shows a mixed signal (Figure 4.17). Monthly rainfall in the Wosha watershed will shift from 23.7% to 9.87% under SSP2-4.5 for CanESM5 in the 2050s. In contrast, SSP5-8.5 will see a change from 23.95% to 3.9% over the same period. For SSP2-4.5, the predicted rainfall from the MIROC6 model showed a change of 32.8% to 12.9% in the 2050s. But under SSP5-8.5, it will shift by 26.1% to

4.2% in the 2050s. The NESM3 model projected that in the 2050s, rainfall would change from 30.3% to 3.9% under the SSP2-4.5 scenario. At the same time, the model showed 31.4% to 2.9% under SSP5-8.5. However, the results show that a climate model is necessary.

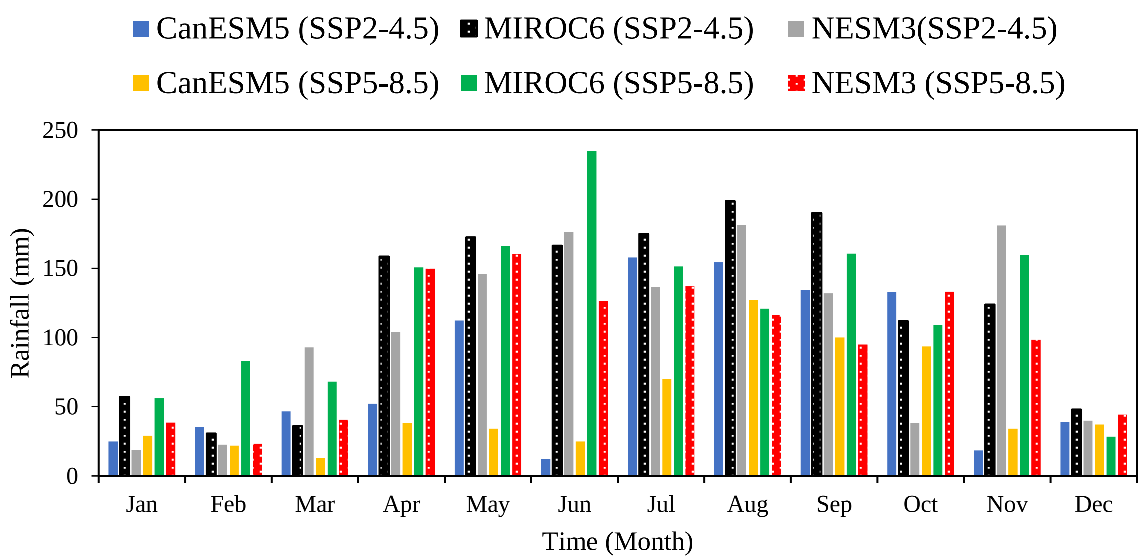

Figure 4.17: Annual Rainfall Change in Mid-Term Scenarios.

The mid-term signals of the simulated monthly maximum temperature have been inconsistent. The monthly maximum temperature of the Wosha watershed will fluctuate by 1.3°c ± 0.1°c from January to December in the 2050s under the MIROC6 and SSP2-4.5 scenarios. On the other hand, throughout the same period, it will rise by 1.4°c ± 0.2°c under SSP5-8.5. The CanESM5 model projected that in the 2050s, the maximum temperature would increase by 1.3°c ± 0.1°c under the SSP2-4.5 scenario. Under SSP5-8.5, it will rise by 1.5°c ± 0.6°c in the 2050s. The 2050s maximum temperature was expected by the NESM3 model to increase by 1.4°c ± 0.2°c under SSP2-4.5. Under SSP5-8.5, the model anticipated 1.5°c ± 0.2°c in the 2050s during the same period (Figure 4.18).

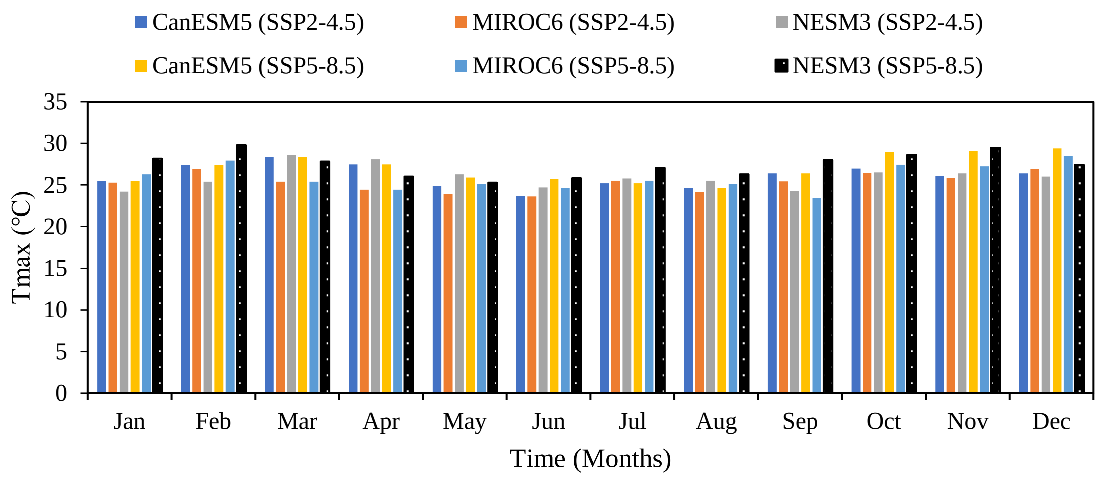

Figure 4.18: Mid-Term Maximum Temperature Change Scenarios.

In the 2050s, the SSP2-4.5 scenario will cause a 1.3°c ± 0.8°c monthly minimum temperature change for MIROC6 in the Wosha watershed from January to December. However, throughout the same period, it will change by 1.2 °c ± 0.2 °c under SSP5-8.5. The CanESM5 model projected that in the 2050s; there would be an increase in minimum temperature of 1.3°c ± 0.4°c, under SSP2-4.5. Under SSP5-8.5, it will also alter by 1.6°c ± 0.6°c in the 2050s. According to the NESM3 model, with SSP2-4.5, the lowest temperature would increase by 0.85°C to 0.2°C in the 2050s. On the other hand, the model anticipated 1.6°c ± 0.2°c under SSP5-8.5 (Figure 4.19).

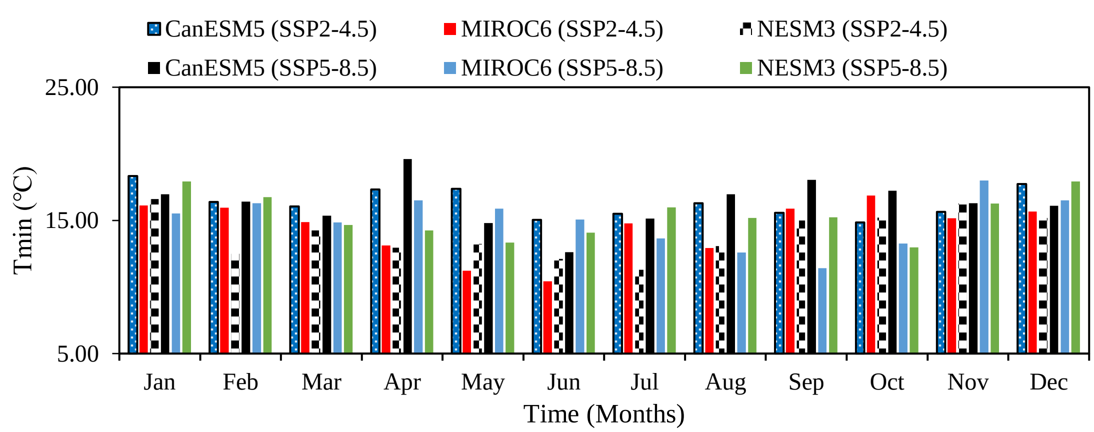

Figure 4.19: The Minimum Temperature in the Mid-Term Change Scenarios.

4.5.3. Long-Term Projected Changes in Annual Rainfall and Temperature.

In the 2080s, the Wosha watershed's monthly rainfall will increase from 27.9% to 31.8% for MIROC6 under SSP2-4.5 (Figure 4.20). In contrast, under SSP5-8.5, it will decrease from 31.6% to 22.8% throughout the same time frame. In the 2080s, under SSP2-4.5, the simulated rainfall from the CanESM5 model showed a decrease from 44.6% to 36.8%. In the 2080s, it will likewise shift from 34.7% to 28.6% under SSP5-8.5. According to the NESM3 model, rainfall in the 2080s will change from 36.9% to 34.6% under SSP2-4.5. Additionally, it demonstrated a decrease under SSP5-8.5 in the 2080s from 38.9% to 24.9%. Additionally, the results obtained here concur with those of other research conducted near the study in the catchment (Edamo, Ukumo, et al., 2022). This study will be a valuable source of knowledge for the Wosha watershed water resource management.

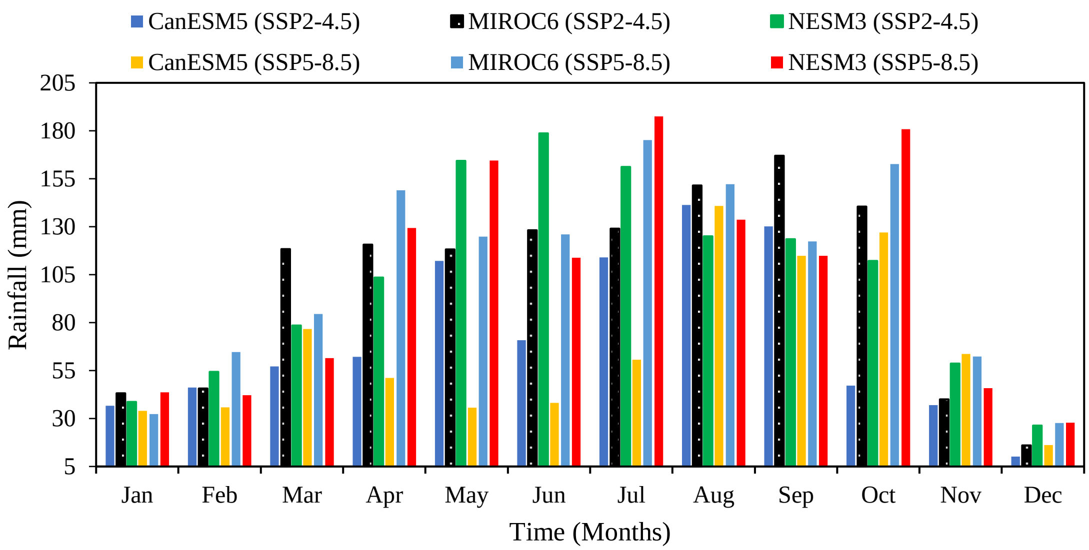

Figure 4.20: Annual Rainfall Change in Lon-Term Scenario

For the model CanESM5 in the 2080s, the Wosha watershed's monthly maximum temperature will vary by 1.4°C ± 0.3°C under SSP2-4.5. Conversely, under SSP5-8.5, it will vary by 1.6 °c ± 0.20 °c in the same time from January to December. The MIROC6 model's simulated maximum temperature showed that, under SSP2-4.5, there would be a 1.7°c ± 0.8°c shift in the 2080s. Additionally, under SSP5-8.5, it will shift by 1.5°c ± 0.26°c in the 2080s. Under SSP2-4.5, the NESM3 model predicted a maximum temperature change of 1.4°c ± 0.2°c in the 2080s. Conversely, the model indicated 1.8°c ± 0.12°c within the same time frame under SSP5-8.5 (Figure 4.21). In the future, the watershed's maximum temperature will climb.

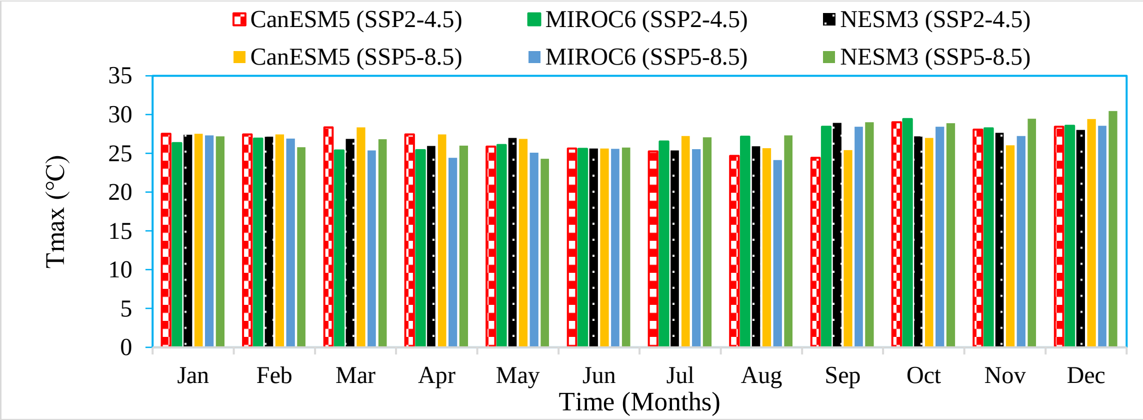

Figure 4.21: Maximum Temperature Change Long-Term Scenario.

The monthly minimum temperature in the Wosha watershed under the SSP2-4.5 scenario, the MIROC6 model projected a shift in the minimum temperature of 1.4°c ± 0.2°c in the 2080s. According to the SSP5-8.5 climate change scenario, it will likewise change by 1.79°c ± 0.2°c in the 2080s. The CanESM5 model projected a 1.6°c ± 0.2°c shift in the 2080s under SSP5-8.5. The model estimated a change of 1.24°c ± 0.6°c under SSP2-4.5 in the 2080s. The NESM3 model projected a minimum temperature increase of 1.8°C to 0.5°C in the 2080s under SSP2-4.5. Additionally, under SSP2-4.5, it displayed a 1.9°c ± 0.2°c increase in the 2080s (Figure 4.22). The watershed's minimum temperature is expected to rise in the medium and long term.

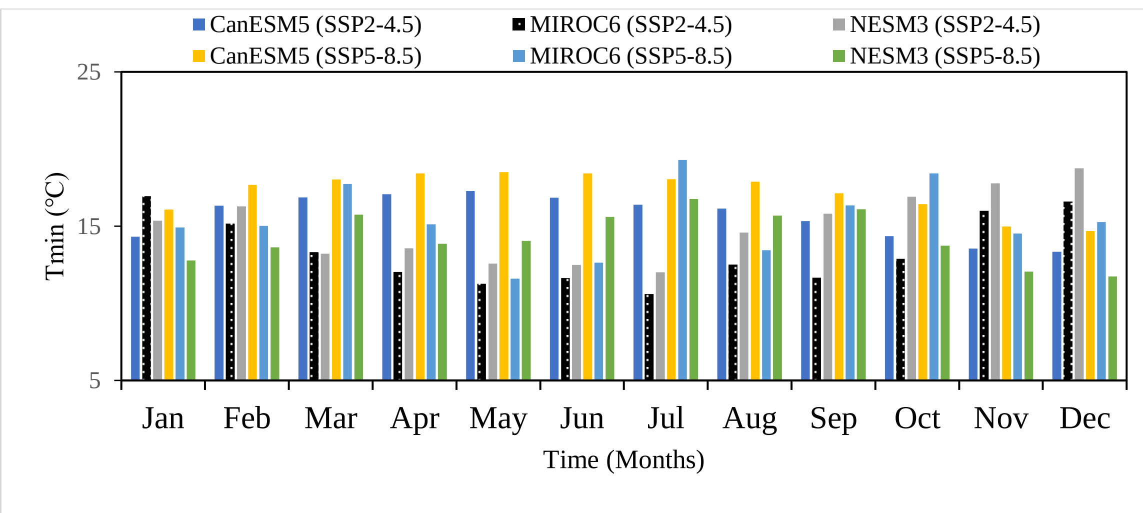

Figure 4.22: Minimum Temperature Change in Long-Term Scenarios.

The Wosha watershed's minimum temperature will rise in the medium and long term. Although it wasn't mentioned specifically for the Wosha watershed, a previous study (Edamo, Ukumo, et al., 2022), also noted an increase in Ethiopia's minimum temperature. The analysis of monthly & annual climatic change relative to baseline results is shown in Appendix A.

4.6. Assessment of the impacts of climate change on the surface water resources in the Wosha watershed

During the baseline period (1985-2014), the analysis of the three climate models—CANESM5, MIROC6, and NESM3—indicates a consistent trend in precipitation and temperature patterns within the Wosha watershed. The models show slight variations in annual precipitation, with CANESM5 predicting the highest average annual precipitation, followed by MIROC6 and NESM3. Temperature trends across all models show a gradual increase, aligning with global warming trends observed in recent decades. These baseline results serve as a critical reference for understanding future climate scenarios and their potential impacts on surface water resources.

4.6.1. Projected seasonal change of precipitation in the Mid-Term Period (2041-2070)

The mid-term projections (2041-2070) demonstrate a significant shift in both precipitation and temperature patterns across the Wosha watershed. CANESM5 predicts a noticeable increase in precipitation during the wet season, which could exacerbate flood risks, while MIROC6 suggests a more moderate increase. MIROC6, however, indicates a potential decrease in precipitation, particularly during the Autumn season (Figure 4.23), which could lead to increased water stress. The temperature rise across all models is more pronounced in this period, with potential implications for evapotranspiration rates and water availability.

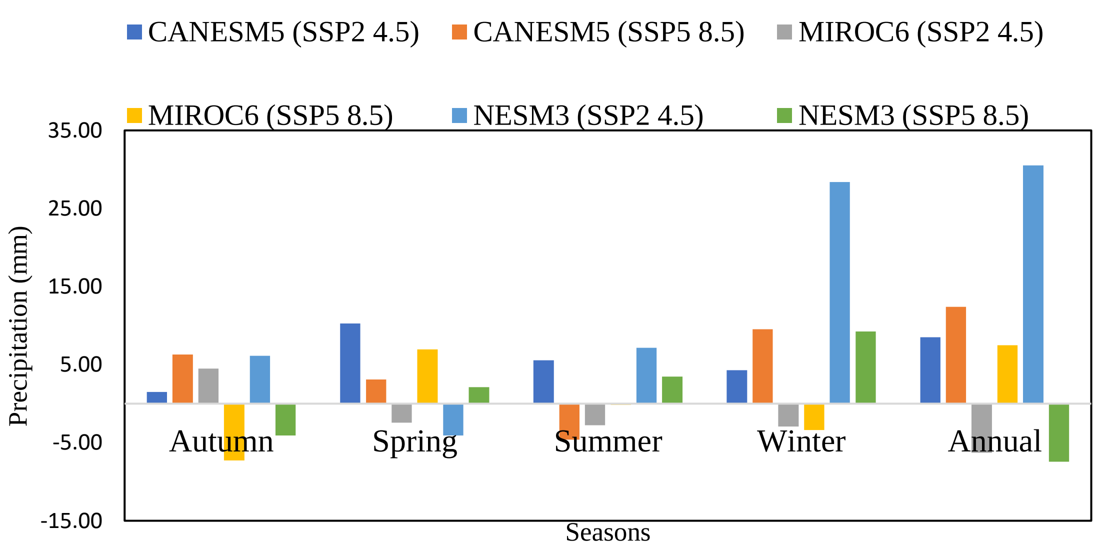

Figure 4.23: Projected precipitation changes in the mid-term period (2041-2070)

In the long-term projections (2071-2100), the models display a more divergent range of outcomes. CANESM5 continues to project a significant increase in precipitation, with potential risks of extreme weather events becoming more frequent. NESM3 shows a stabilization in precipitation levels, suggesting that the changes might not be as severe as other models predict (Figure 4.24). MIROC6, on the other hand, indicates a further decline in precipitation, potentially leading to prolonged drought periods. The temperature increase is consistent across all models, with the most extreme changes predicted by CANESM5, indicating a possible escalation in the challenges posed by climate change on water resources.

4.6.2. Projected seasonal change in precipitation in long-term period (2071-2100)

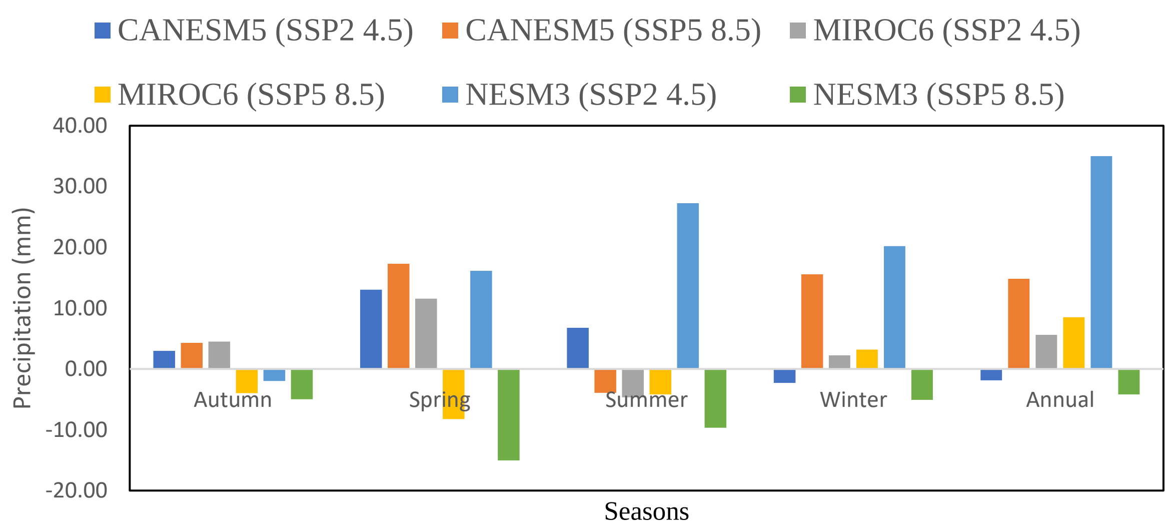

Figure 4.24: Projected precipitation changes in long-term period (2071-2100)

4.6.3. Projected seasonal streamflow changes in Mid-term 2050s (2041-2070)

The projected seasonal streamflow changes in the mid-term period are shown in Figure 4.25. Almost all the models showed a decline in streamflow in the 2050s. The highest available streamflow is simulated by the CanESM5 model in the summer season (14.222 m^3/s).

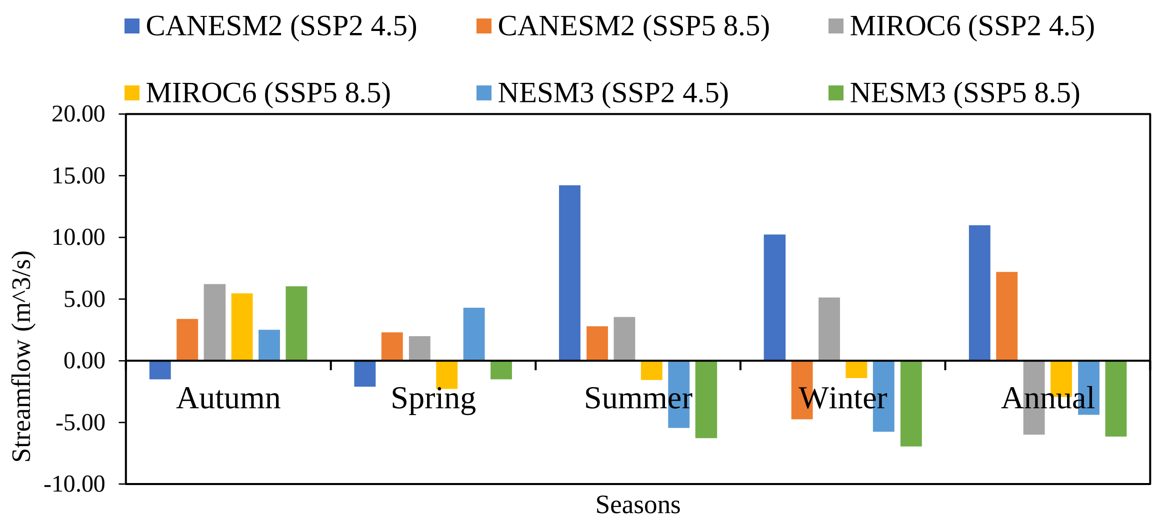

Figure 4.25: Projected stream flow changes in the mid-term period (2041-2070)

4.6.4. Projected changes in stream flow in long-term 2080s (2071-2100)

The stream flow change in the long-term or 2080s is shown in Figure 4.26. CanESM5 model estimated 26.97 m^3/s stream flow in the summer season under SSP5 8.5.

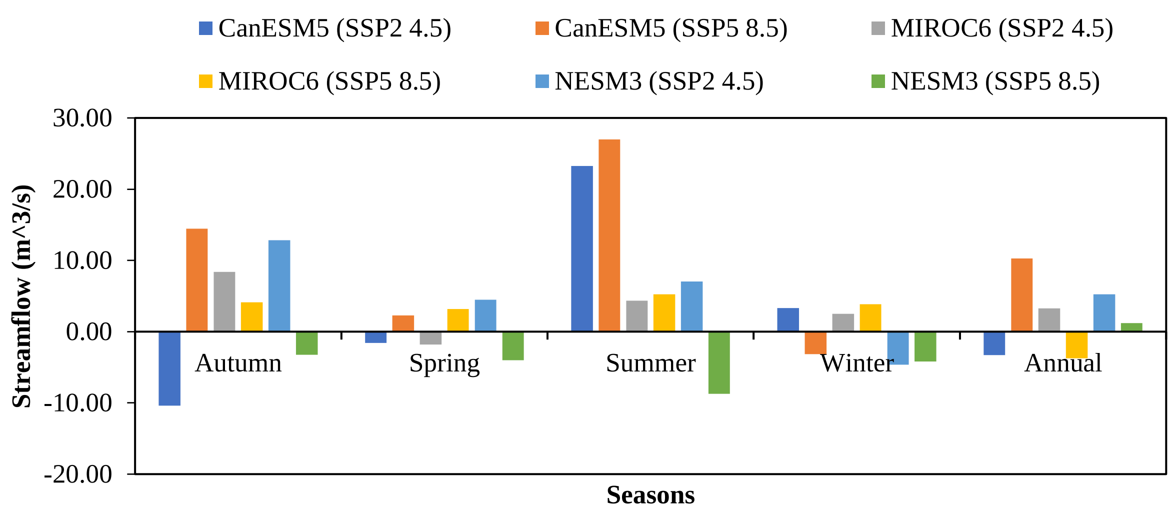

Figure 4.26: Projected stream flow changes in a long-term period (2071-2100)

Comparative Analysis of Models

When comparing the three models, CANESM5 tends to project the most extreme changes in both precipitation and temperature, suggesting a scenario with higher variability in water resources. MIROC6 provides a more conservative estimate, with changes being less drastic, which could imply a more manageable adaptation scenario. NESM3, with its predictions of decreasing precipitation, especially in the long term, highlights the potential for significant drought-related challenges. This variability across models underscores the uncertainty inherent in climate projections and the need for flexible and adaptive management strategies.

4.7. Biophysical and socio-economic problems of the watershed for different land uses classes

4.7.1. Accuracy Assessment

The most common way to assess the accuracy of a classified map is to create a set of random points from the ground truth data and compare that to the classified data in a confusion matrix (Table 4.10). Although this is a two-step process, you may need to compare the results of different classification methods or training sites, or you may not have ground truth data and are relying on the same imagery that you used to create the classification.

Table 4.10: Accuracy Assessment

	water	Grasses	Shrubland	Forest	Wetland	Pasture	Agricultural land	Total user
Water	4	0	0	0	0	0	0	4
Grasses	0	6	1	0	0	0	0	7
Shrubland	0	2	7	0	0	1	1	8
Forest	0	0	0	4	0	0	0	4
Wetland	0	0	0	0	2	1	0	2
Pasture	0	1	1	0	1	5	3	9
Agricultural and	0		1	0	0	4	5	8
Total Producer	4	9	7	4	2	9	7	35

The area coverage changes in LULC for years 1997, 2008 and 2017 is described in Table 4.11.

Table 4.11: Area of Land use Land cover of (1997, 2008, 2017)

Class name	**Area 1997(%)**	**Class name**	**Area (%)2008**	**Class name**	**Area (%) 2017**
Agricultural land	10.51	Agricultural land	9.84	Agricultural land	15.92
Pasture	14.20	Pasture	16.05	Pasture	10.73
Wetland	3.91	Wetland	14.48	Wetland	3.40
Forest	6.66	Forest	14.72	Forest	7.34
Shrubland	6.23	Shrubland	4.68	Shrubland	3.22
Grasses	58.07	Grasses	39.58	Grasses	59
Water	0.42	Water	0.64	Water	0.38
Total	**100%**		**100%**		**100%**

The land use land cover maps of the Wosha watershed are shown in Figure 4.27.

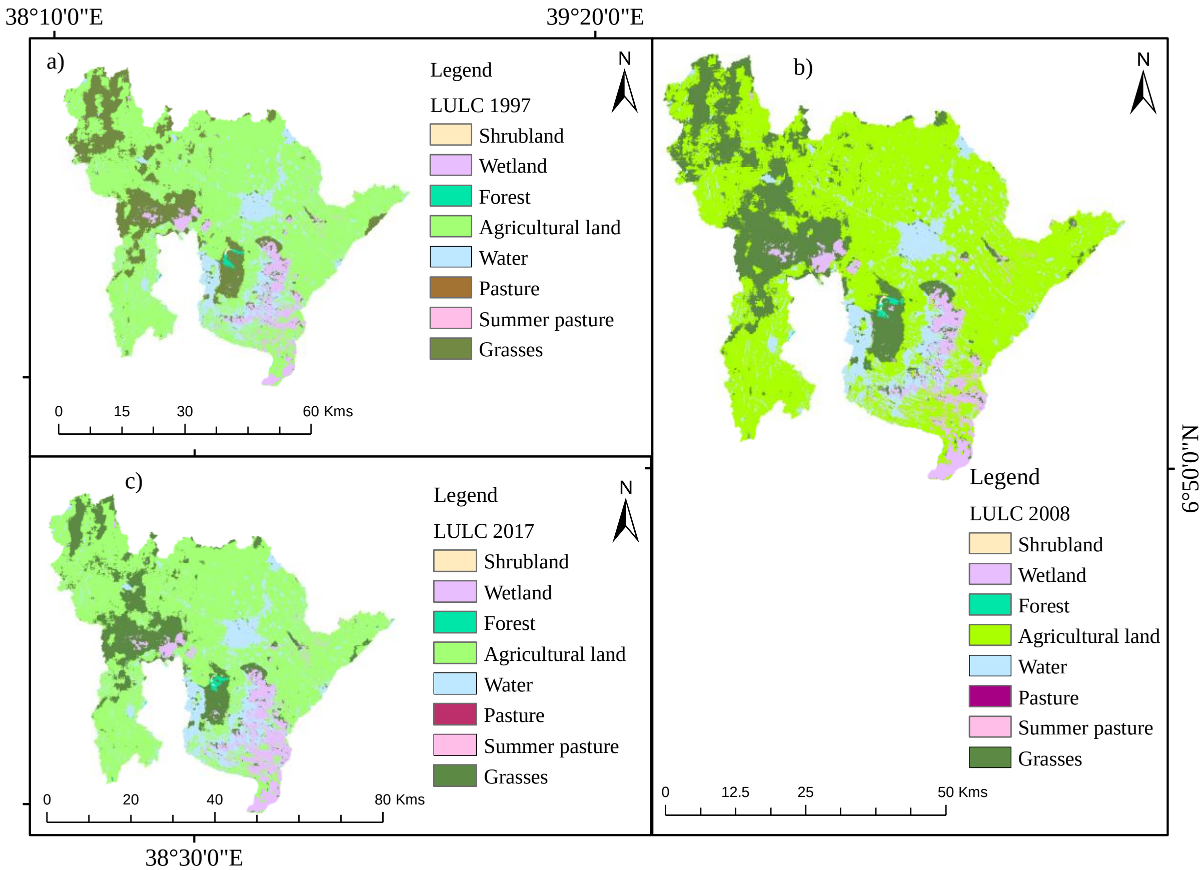

Figure 4.27: Land Use/ Cover changes over the period a) 1997, b) 2008, and c) 2017 in Wosha watershed

4.7.2. Prediction of Land Use Land Cover

After classification of land use land cover of three decades in this study 2067 was used prediction of future of LULC in order to compare the previous maps. MOLUSCE tool in QGIS (3.14.16) is used for this purpose. In our future climate projection long term is 2050s and 2080s, so we want to compare the future impacts of land use land cover in surface water availability. The watershed's water resources were found to be increasingly scarce, particularly during the dry season. Changes in land use, coupled with altered precipitation patterns due to climate change, contributed to reduced surface water availability.

The significant projects changes in LULC for the period 2080 is shown in Figure 4.28.

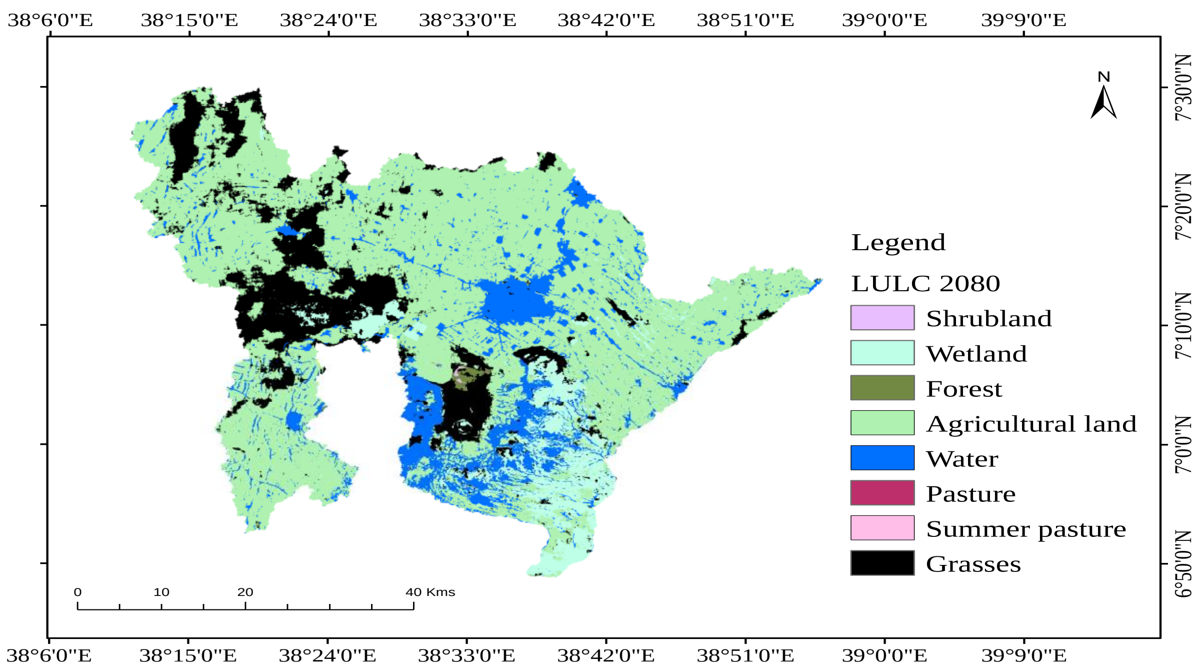

Figure 4.28: Land Use/ Cover changes over the projected period of 2080 in Wosha watershed

The biophysical and socio-economic problems identified in the Wosha watershed are interrelated and reflective of broader issues related to land use changes and climate variability. The findings highlight the critical need for integrated watershed management strategies that address both environmental and socio-economic dimensions. The degradation of soil and vegetation, coupled with increased water scarcity, underscores the importance of implementing sustainable land management practices. Soil conservation measures, reforestation, and improved land use planning are essential to mitigate erosion and enhance water retention. Additionally, adaptive measures to cope with changing precipitation patterns can help improve water resource management.

The adverse effects on agriculture and health indicate a pressing need for community-based adaptation strategies. Training programs for farmers on sustainable agricultural practices and the development of infrastructure for improved water supply and sanitation can help alleviate some of the socio-economic challenges. Furthermore, economic support mechanisms and policy interventions are necessary to assist affected communities in coping with the financial impacts of climate change and land use changes. Overall, addressing the biophysical and socio-economic problems in the Wosha watershed requires a holistic approach that integrates environmental conservation with socio-economic development to ensure sustainable and resilient communities.

4.8. Comparison of the findings of this thesis with previous studies

There is no previous study in Wosha on water availability under climate change impacts. But we try to compare results in thesis of climate change and land use land cover changes on surface hydrology in Ethiopia and across the globe.

The findings of this thesis on the Wosha watershed in the Rift Valley Lakes Basin of Ethiopia reveal significant impacts of climate change on water availability. Using advanced hydrological models and climate projections, the study demonstrates that rising temperatures and changes in precipitation patterns are leading to increased evapotranspiration and altered streamflow regimes. This results in reduced water availability during critical periods, such as the dry season, affecting both agricultural productivity and water supply for local communities. The study also highlights an increase in the frequency and intensity of extreme weather events, such as droughts and floods, further complicating water management strategies in the region.

Comparatively, previous studies in similar watersheds within Ethiopia and other parts of Sub-Saharan Africa have also identified climate change as a significant factor impacting water resources (Ayele et al., 2022; Edamo, Bushira, et al., 2022; Ukumo, Edamo, et al., 2022). However, earlier research often emphasized general trends in precipitation and temperature changes without providing detailed insights into specific hydrological processes (Dagnachew et al., 2024). This thesis adds value by focusing on the Wosha watershed, employing high-resolution climate data and state-of-the-art modeling techniques to produce more localized and accurate predictions of water availability under SSP2 4.5 and SSP5 8.5. Unlike some earlier studies that predominantly relied on historical data, this research integrates both historical observations and future climate scenarios, providing a more comprehensive understanding of potential changes in water resources (Dalle et al., 2023).

Moreover, this thesis aligns with and expands upon recent studies that have begun to examine the compound effects of climate change and land use changes on water resources. While previous research has often treated these factors independently, the findings here underscore the importance of considering their combined impact. The study reveals that land degradation and deforestation, coupled with climate change, exacerbate water scarcity issues. This comprehensive approach provides a more nuanced understanding of water resource challenges in the Wosha watershed , emphasizing the need for integrated management strategies that address both climate change and human-induced factors (Idrissou et al., 2022).

A research made by Negash (2014) shows that the hydrology of the Bilate watershed is greatly impacted by changes in land use and land cover (LULC). Agricultural and urban areas increased by 8.75% and 4.58%, respectively, between 1994 and 2009, whereas woodland and forest lands decreased by 6.29% and 4.08%, in line with this trend. Surface runoff (Qs) and evapotranspiration (ET) rose by 11.97% and 0.51%, respectively, as a result of these modifications. RCP4.5 and RCP8.5 climate change scenarios predicted increases in temperatures of 1.87°C and 2.29°C, respectively, and decreases in rainfall of 9.5% and 12.17%, respectively. As a result, evapotranspiration rose by 4.7% and surface runoff reduced by 14.59%. The combined effects of climate change and LULC showed a 5.39% drop in surface runoff and evapotranspiration. The authors focused on RCPs to forecast future climate changes and avoided SSPs. The studies' calibration and validation procedures showed good model performance, with high R^2 and NSE values indicating trustworthy simulations of the hydrological processes occurring in the corresponding watershed. The future climate scenarios would likely result in higher temperatures and precipitation than baseline times, highlighting the necessity of better water management strategies to prepare for these changes. The contribution lies of changes with climate projections to evaluate their combined influence on water resources is a significant contribution to the discipline. With a more thorough understanding of the various elements influencing water availability, this holistic approach offers stakeholders and policymakers insightful information for creating sustainable water management plans. A practical component of the study is further added by the in-depth seasonal examination of streamflow fluctuations, which addresses practical implications for managing water resources in the face of climate change.

5. CONCLUSION AND RECOMMENDATION

5.1. CONCLUSION

The interconnectedness of hydrology, climate science, and predictive modeling underscores the need for comprehensive and forward-thinking approaches to water resource management. This research utilized climate models such as CanESM5, MIROC6, and NESM3 to analyze climate change effects over three distinct periods: the baseline (1985-2014), the 2050s, and the 2080s. By employing the SWAT model for rainfall-runoff simulations, we generated projections of future stream flow and assessed potential variations in rainfall and temperature.

Based on SWAT model watershed delineation, the Wosha watershed the catchment area is 2848.3 km^2. Overlaying land use, soil and slope were performed to generate HRUs. Climatic data from January 1988 - December 2023 were inputs during SWAT model simulation. The calibration and validation carried out from January 2001 to December 2010 and January 2011 - December 2015 respectively on monthly basis of stream flow data using automatic calibration with Sequential Uncertainty Fitting (SUFI-2) in SWAT- CUP.

Model performance efficiency was checked by coefficient of determination (R^2) and Nash-Sutcliffe model efficiency (NSE). Accordingly, the values of R^2 and NSE were 0.77 & 0.75 and 0.8 and 0.72 respectively during calibration and validation period for stream flow.

These the mentioned results depicted that model was well reasonably simulated the discharge and sediment yield from Gidabo watershed.

The findings indicated that climate change could significantly impact water availability in the Wosha watershed. In the 2050s, annual rainfall is projected to vary by ±25.38% under the SSP2 4.5 scenario and by ±8.3% under the SSP5 8.5 scenario. By the 2080s, these projections change to ±11.12% for SSP2 4.5 and ±33.43% for SSP5 8.5. Correspondingly, annual stream flow is expected to change by ±12.97% under SSP2 4.5 and ±5.10% under SSP5 8.5 in the 2050s, with further changes of ±37.30% and ±22.7% anticipated by the 2080s, respectively.

Utilizing multiple climate models allowed for a robust comparison of hydrological estimates at the watershed level, enhancing the reliability of our projections compared to single-model approaches. However, it is important to note that while the use of multiple model ensembles is promising, their application in assessing water resource potential in key catchments under changing climate scenarios remains largely unexamined in both Ethiopia and globally. This study highlights the necessity for further exploration in this area to fully understand and address the implications of climate change on water resources.

5.2. Recommendation

Based on the findings regarding the impacts of climate change on water availability in the Wosha watershed, the following recommendations are proposed to enhance resilience and ensure sustainable water resource management:

- **Implement Integrated Water Resources Management (IWRM)**

Adopting an IWRM framework will facilitate coordinated management of water, land, and related resources. This approach should involve all stakeholders, including local communities, government agencies, and NGOs, to ensure equitable and sustainable use of water resources.

- **Promote Rainwater Harvesting and Storage Solutions**

Encouraging the construction of rainwater harvesting systems can significantly enhance water availability during dry periods. Additionally, developing small-scale reservoirs and water storage facilities will help manage seasonal variations in water supply and mitigate the impacts of extreme weather events.

- **Enhance Agricultural Resilience**

Supporting farmers in adopting climate-smart agricultural practices is crucial. This includes promoting drought-tolerant crop varieties, implementing agroforestry, and providing training on sustainable farming techniques that improve soil health and water retention.

- **Strengthen Soil Conservation Practices**

To combat soil erosion and enhance agricultural productivity, practices such as terracing, contour farming, and cover cropping should be promoted. These methods will improve water infiltration and reduce runoff, contributing to better water management.

- **Restore and Protect Ecosystems**

Restoration of wetlands and reforestation of degraded areas within the watershed will improve biodiversity and enhance ecosystem services, such as natural flood control and water purification. These initiatives should be integrated into land use planning.

- **Community Engagement and Education**

Building local capacity through educational programs on climate change impacts and sustainable practices is essential. Engaging communities in decision-making processes will ensure that adaptation strategies are culturally relevant and effectively implemented.

- **Establish Continuous Monitoring Systems**

Implementing a robust monitoring system for hydrological changes and climate impacts will provide valuable data to inform adaptive management strategies. This system should include the use of technology for real-time data collection and analysis.

- **Support Research and Development Initiatives**

Investing in research focused on the specific challenges of the Wosha watershed is vital. This includes developing and validating hydrological models that incorporate climate change scenarios and assessing their implications for water resource management.

- **Develop Adaptive Policies and Secure Funding**

Creating flexible policies that can be adjusted according to new climate data and hydrological assessments is critical. Furthermore, securing funding for adaptation projects will ensure the sustainability and resilience of water resources in the watershed.

By implementing these recommendations, stakeholders in the Wosha watershed can effectively address the challenges posed by climate change, enhance water resource management, and promote sustainable development in the watershed.

REFERENCES

Abdollahbeigi, M. (2020). Non-Climatic Factors Causing Climate Change. Journal of Chemical Reviews, 2(4), 292–308. http://www.jchemrev.com/article_118056.html

Ahmad, S., Khan, I.H., Parida, B.P. (2001). Performance of stochastic approaches for forecasting river water quality. Water Research. 35: 4119-4266.

Arnold J.G. Srinivasan R.S. Muttiah, and J.R. Williams. (1998). Large area hydrologic modeling and assessment part I: model development. J. American Water Resources Association, 34(1),73-89.

Asempah, M., Shisanya, C. A., & Schütt, B. (2024). Modeling of soil erosion risk in a typical tropical savannah landscape. Scientific African, 23(December 2023), e02042. https://doi.org/10.1016/j.sciaf.2023.e02042

Aversa, D. (2023). Scenario analysis and climate change: a literature review via text analytics. British Food Journal, 126(1), 271–289. https://doi.org/10.1108/BFJ-08-2022-0691

Ayehu, G. T., Tadesse, T., Gessesse, B., & Dinku, T. (2018). Validation of new satellite rainfall products over the Upper Blue Nile Basin, Ethiopia. Atmospheric Measurement Techniques, 11(4), 1921–1936. https://doi.org/10.5194/amt-11-1921-2018

Ayele, M. A., Lohani, T. K., Mirani, K. B., Edamo, M. L., & Ayalew, A. T. (2022). Simulating sediment yield by SWAT and optimizing the parameters using SUFI-2 in Bilate river of Lake Abaya in Ethiopia. World Journal of Engineering, ahead-of-p(ahead-of-print). https://doi.org/10.1108/wje-07-2021-0449

Bekele, A. A., Pingale, S. M., Hatiye, S. D., & Tilahun, A. K. (2019). Impact of climate change on surface water availability and crop water demand for the sub-watershed of Abbay Basin, Ethiopia. Sustainable Water Resources Management, 5(4), 1859–1875. https://doi.org/10.1007/s40899-019-00339-w

Bergström, S. (1995). The HBV model. Computer models of watershed hydrology. Water Resources Publications, Colorado, 443-476.

Beven, K. (2000). Rainfall-Runoff model: the primer/Keith Beven.-2nd ed. Lancaster University, UK.

Birhanu, T. (2015). Flood Mitigation Alternatives For Selected Reachs Of Awash River From

Logiya To Dubti.

Boru, G. F., Gonfa, Z. B., & Diga, G. M. (2019). Impacts of climate change on stream flow and water availability in Anger sub-basin, Nile Basin of Ethiopia. Sustainable Water Resources Management, 5(4), 1755–1764. https://doi.org/10.1007/s40899-019-00327-0

Casanueva, A., Kotlarski, S., Herrera, S., Fernández, J., Gutiérrez, J. M., Boberg, F., Colette, A., Christensen, O. B., Goergen, K., Jacob, D., Keuler, K., Nikulin, G., Teichmann, C., & Vautard, R. (2016). Daily precipitation statistics in a EURO-CORDEX RCM ensemble: added value of raw and bias-corrected high-resolution simulations. Climate Dynamics, 47(3–4), 719–737. https://doi.org/10.1007/s00382-015-2865-x

Chen, J., Cui, H., Xu, Y., & Ge, Q. (2021). Long-term temperature and sea-level rise stabilization before and beyond 2100: Estimating the additional climate mitigation contribution from China's recent 2060 carbon neutrality pledge. Environmental Research Letters, 16(7). https://doi.org/10.1088/1748-9326/ac0cac

Chow, V.T., Maidment, D.R., Mays, L.W. (1988). Applied Hydrology. McGraw-Hill: New York, USA.

Chuderlik. (2003). hydrological model selection for CFCAS project, assessement of water resources risk and vunerability to changing climate conditions , project report I. 40pp.

Dagnachew, C., Abebe, A., Mohammed, K., Yisihak, T., & Legesse, M. (2024). Evaluation of hydraulic adequacy of runoff disposal in urban watersheds of rapidly expanding towns. 7(3), 243–271. https://doi.org/10.2166/h2oj.2024.095

Dalle, D., Gecho, Y., & Bedeke, S. B. (2023). Spatiotemporal Variability and Trends in Rainfall and Temperature in South Ethiopia: Implications for Climate Change Adaptations in Rural Communities. Advances in Meteorology, 2023. https://doi.org/10.1155/2023/1939528

Dubovský, V., Dlouhá, D., & Pospíšil, L. (2021). The calibration of evaporation models against the penman-monteith equation on lake most. Sustainability (Switzerland), 13(1), 1–17. https://doi.org/10.3390/su13010313

Edamo, M. L., Bushira, K. M., Ukumo, T. Y., Ayele, M. A., Alaro, M. A., & Borko, H. B. (2022). Effect of climate change on water availability in Bilate catchment, Southern Ethiopia. Water

Cycle, 3(June), 86–99. https://doi.org/10.1016/j.watcyc.2022.06.001

Edamo, M. L., Ukumo, T. Y., Lohani, T. K., & Mirani, K. B. (2022). Flood inundation mapping under climate change scenarios in the Boyo watershed of Muluneh Legesse Edamo. 13(8), 3170–3188. https://doi.org/10.2166/wcc.2022.193

Folland, C. K., Karl, T. R., & Vinnikov, K. Y. (1990). Observed climate variations and change. Climate Change: The IPCC Scientific Assessment, 195–238.

Girma, M. M. (2012). Potential Impact of Climate and Land Use Changes on the Water Resources of the upper Blue Nile Basin.

Haan, C. T., Barfield, B.J. & Hayes, J.C. (1994). Design Hydrology and Sedimentology for Small Watersheds. Academic Press, San Diego, CA. pp 588 .

Haile, B. T., Zeleke, T. T., Beketie, K. T., Ayal, D. Y., & Feyisa, G. L. (2021). Analysis of El Niño Southern Oscillation and its impact on rainfall distribution and productivity of selected cereal crops in Kembata Alaba Tembaro zone. Climate Services, 23, 100254. https://doi.org/10.1016/j.cliser.2021.100254

He, L., Duan, X., Ding, S., Cai, C., & Deng, Y. (2023). Construction and evaluation of pedotransfer functions for saturated hydraulic conductivity in the granite red soil regions of southern China. Journal of Hydrology: Regional Studies, 50(June), 101539. https://doi.org/10.1016/j.ejrh.2023.101539

Idrissou, M., Diekkrüger, B., Tischbein, B., de Hipt, F. O., Näschen, K., Poméon, T., Yira, Y., & Ibrahim, B. (2022). Modeling the Impact of Climate and Land Use/Land Cover Change on Water Availability in an Inland Valley Catchment in Burkina Faso. Hydrology, 9(1). https://doi.org/10.3390/hydrology9010012

IPCC. (2023a). Impacts, Adaptation, and Vulnerability. Working Group II Contribution to the IPCC Sixth Assessment Report of the Intergovernmental Panel on Climate Change; Pötner, H. In O., Roberts, DC, Tignor, M., Poloczanska, ES, Mintenbeck, K., Ale, A., Eds. https://doi.org/10.1017/9781009325844.Front

IPCC. (2023b). Summary for Policymakers: Synthesis Report. Climate Change 2023: Synthesis Report. Contribution of Working Groups I, II and III to the Sixth Assessment Report of the

Intergovernmental Panel on Climate Change, 1–34.

Jin, H., Jiang, W., Chen, M., Li, M., Bakar, K. S., & Shao, Q. (2023). Downscaling long lead time daily rainfall ensemble forecasts through deep learning. Stochastic Environmental Research and Risk Assessment, 37(8), 3185–3203. https://doi.org/10.1007/s00477-023-02444-x

Kc, S. (2024). Updating the Shared Socioeconomic Pathways (SSPs) Global Population and Human Capital Projections Approved by : February, 1–78.

Keller, A. A., Garner, K. L., Rao, N., Knipping, E., & Thomas, J. (2022). Downscaling approaches of climate change projections for watershed modeling: Review of theoretical and practical considerations. PLOS Water, 1(9), e0000046. https://doi.org/10.1371/journal.pwat.0000046

Kim, J., Waliser, D. E., Mattmann, C. A., Goodale, C. E., Hart, A. F., Zimdars, P. A., Crichton, D. J., Jones, C., Nikulin, G., Hewitson, B., Jack, C., Lennard, C., & Favre, A. (2014). Evaluation of the CORDEX-Africa multi-RCM hindcast: Systematic model errors. Climate Dynamics, 42(5–6), 1189–1202. https://doi.org/10.1007/s00382-013-1751-7

Kopp, R. E., Oppenheimer, M., O'Reilly, J. L., Drijfhout, S. S., Edwards, T. L., Fox-Kemper, B., Garner, G. G., Golledge, N. R., Hermans, T. H. J., Hewitt, H. T., Horton, B. P., Krinner, G., Notz, D., Nowicki, S., Palmer, M. D., Slangen, A. B. A., & Xiao, C. (2023). Communicating future sea-level rise uncertainty and ambiguity to assessment users. Nature Climate Change, 13(7), 648–660. https://doi.org/10.1038/s41558-023-01691-8

Krinner, G., Germany, F., Shongwe, M., Africa, S., France, S. B., Uk, B. B. B. B., Germany, V. B., Uk, O. B., France, C. B., Uk, R. C., Canada, M. E., Erich, M., Uk, R. W. L., Uk, S. L., & Lucas, C. (2013). Long-term climate change: Projections, commitments and irreversibility. Climate Change 2013 the Physical Science Basis: Working Group I Contribution to the Fifth Assessment Report of the Intergovernmental Panel on Climate Change, 9781107057, 1029–1136. https://doi.org/10.1017/CBO9781107415324.024

Kuma, H. G., Feyessa, F. F., & Demissie, T. A. (2021). Hydrologic responses to climate and land-use/land-cover changes in the Bilate catchment, southern Ethiopia. Journal of Water and Climate Change, 12(8), 3750–3769. https://doi.org/10.2166/wcc.2021.281

Kundzewicz, Z. W., Kanae, S., Seneviratne, S. I., Handmer, J., Nicholls, N., Peduzzi, P., Mechler, R., Bouwer, L. M., Arnell, N., Mach, K., Muir-Wood, R., Brakenridge, G. R., Kron, W., Benito, G., Honda, Y., Takahashi, K., & Sherstyukov, B. (2014). Le risque d'inondation et les perspectives de changement climatique mondial et régional. Hydrological Sciences Journal, 59(1), 1–28. https://doi.org/10.1080/02626667.2013.857411

Ly, S., Charles, C., & Degré, A. (2011). Geostatistical interpolation of daily rainfall at catchment scale: The use of several variogram models in the Ourthe and Ambleve catchments, Belgium. Hydrology and Earth System Sciences, 15(7), 2259–2274.

Moges, E., Demissie, Y., Larsen, L., & Yassin, F. (2021). Review: Sources of hydrological model uncertainties and advances in their analysis. Water (Switzerland), 13(1), 1–23. https://doi.org/10.3390/w13010028

Negash, W. (2014). Catchment dynamics and its impact on runoff generation: Coupling watershed modelling and statistical analysis to detect catchment responses. International Journal of Water Resources and Environmental Engineering, 6(2), 73–87. https://doi.org/10.5897/ijwree2013.0449

Neitsch, S. ., Arnold, J. ., Kiniry, J. ., & Williams, J. . (2011). Soil & Water Assessment Tool Theoretical Documentation Version 2009. Texas Water Resources Institute, 1–647. https://doi.org/10.1016/j.scitotenv.2015.11.063

Nica, A., Popescu, A., & Ibanescu, D.-C. (2019). Human Influence on the Climate System. Current Trends in Natural Sciences, 8(15), 209–215. http://www.natsci.upit.ro

Orke, Y. A., & Li, M. H. (2021). Hydroclimatic variability in the bilate watershed, ethiopia. Climate, 9(6). https://doi.org/10.3390/cli9060098

Paranunzio, R., Anton, I., Adirosi, E., Ahmed, T., Baldini, L., Brandini, C., Giannetti, F., Meulenberg, C., Ortolani, A., Pilla, F., Iglesias, G., & Gharbia, S. (2023). A New Approach towards a User-Driven Coastal Climate Service to Enhance Climate Resilience in European Cities. Sustainability, 16(1), 335. https://doi.org/10.3390/su16010335

Pielke, R., Burgess, M. G., & Ritchie, J. (2022). Plausible 2005-2050 emissions scenarios project between 2 °c and 3 °c of warming by 2100. Environmental Research Letters, 17(2). https://doi.org/10.1088/1748-9326/ac4ebf

Stewart-Koster, B., Bunn, S. E., Green, P., Ndehedehe, C., Andersen, L. S., Armstrong McKay, D. I., Bai, X., DeClerck, F., Ebi, K. L., Gordon, C., Gupta, J., Hasan, S., Jacobson, L., Lade, S. J., Liverman, D., Loriani, S., Mohamed, A., Nakicenovic, N., Obura, D., … Zimm, C. (2023). Living within the safe and just Earth system boundaries for blue water. Nature Sustainability, 7(January). https://doi.org/10.1038/s41893-023-01247-w

Sulamo, M. A., Kassa, A. K., & Roba, N. T. (2021). Evaluation of the impacts of land use/cover changes on water balance of bilate watershed, rift valley basin, ethiopia. Water Practice and Technology, 16(4), 1108–1127. https://doi.org/10.2166/wpt.2021.063

Tadese, Lalit Kumar, Richard Koech, Benjamin K. Kogo (2020). Mapping of land-use/land-cover changes and its dynamics in Awash River Basin using remote sensing and GIS, Remote Sensing Applications: Society and Environment, Volume 19.

Tariq, M., Khan, M. A., Muhammad, W., & Ahmad, S. (2023). Fiber Crops in Changing Climate. In Global Agricultural Production: Resilience to Climate Change. https://doi.org/10.1007/978-3-031-14973-3_9

Ukumo, T. Y., Edamo, M. L., Abdi, D. M., & Derebe, M. A. (2022). Evaluating water availability under changing climate scenarios in the Woybo catchment, Ethiopia. Journal of Water and Climate Change, 13(11), 4130–4149. https://doi.org/10.2166/wcc.2022.343

Ukumo, T. Y., Lohani, T. K., Edamo, M. L., Alaro, M. A., Ayele, M. A., & Borko, H. B. (2022). Application of Regional Climatic Models to Assess the Performance Evaluation of Changes on Flood Frequency in Woybo. 2022.

US-ACE. (2001). Hydrologic Modeling System HEC-HMS. User's Manual, Version 2.1. US Army Corps of Engineers, Hydrologic Engineering Center, pp 178.

Von Uexkull, N., & Buhaug, H. (2021). Security implications of climate change: A decade of scientific progress. Journal of Peace Research, 58(1), 3–17. https://doi.org/10.1177/0022343320984210

Williams, J. (1995). The EPIC Model: In Computer Models of Watershed Hydrology. Water Resources Publications. Highlands Ranch, CO., p. 909-1000.

Yersaw, B. T., & Chane, M. B. (2024). Regional climate models and bias correction methods for rainfall - runoff modeling in Katar watershed , Ethiopia. Environmental Systems Research. https://doi.org/10.1186/s40068-024-00340-z

APPENDICES

Appendix A The analysis of monthly & annual climatic change relative to baselines.

Model	Period	SSP	Element	Monthly	Annual

CanESM5	2050s	2-4.5	Rainfall (%)	8.9	5.3
			Tmax (°C)	1.4	1.72
			Tmin (°C)	1	1.2
		5-8.5	Rainfall (%)	0.9	14.9
			Tmax (°C)	1.6	0.8
			Tmin (°C)	1.1	1.3
	2080s	2-4.5	Rainfall (%)	-2	-1.9
			Tmax (°C)	0.8	1.07
			Tmin (°C)	1.16	1.41
		5-8.5	Rainfall (%)	25.7	16.6
			Tmax (°C)	0.7	0.4
			Tmin (°C)	1.15	2.6
MIROC6	2050s	2-4.5	Rainfall (%)	18.8	5.8
			Tmax (°C)	0.5	0.53
			Tmin (°C)	1.2	0.42
		5-8.5	Rainfall (%)	11.4	9.3
			Tmax (°C)	1.2	0.34
			Tmin (°C)	1.28	2.7
	2080s	2-4.5	Rainfall (%)	11.2	4.3
			Tmax (°C)	1.01	0.7
			Tmin (°C)	1.32	2.9
		5-8.5	Rainfall (%)	15.9	7.3
			Tmax (°C)	1.6	0.2
			Tmin (°C)	1	2.7
NESM3	2050s	2-4.5	Rainfall (%)	24.6	20.3
			Tmax (°C)	1.13	0.5
			Tmin (°C)	1.43	0.7
		5-8.5	Rainfall (%)	26.2	21.1
			Tmax (°C)	1.63	1.7
			Tmin (°C)	1.3	0.9
	2080s	2-4.5	Rainfall (%)	12.4	3.2
			Tmax (°C)	1.42	0.3
			Tmin (°C)	1	0.6
		5-8.5	Rainfall (%)	12.4	6.3
			Tmax (°C)	1.21	0.3
			Tmin (°C)	1.33	0.5

Mann Kendall Trend Test

Rainfall

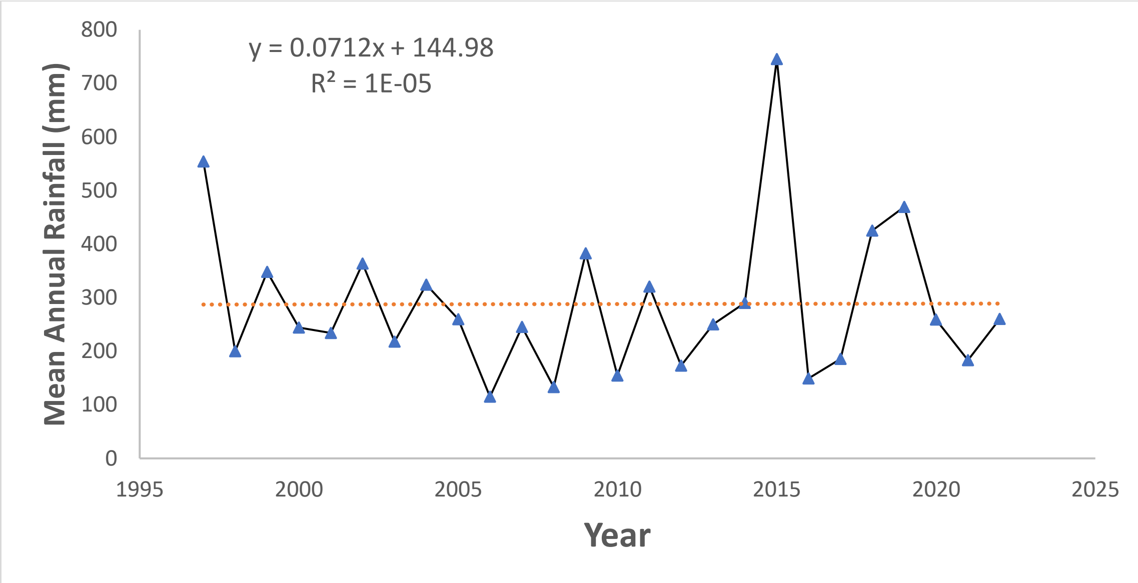
y = 0.0712x + 144.98
R^2 = 1E-05
Mean Annual Rainfall (mm)
800
700
600
500
400
300
200
100
0
1995
2000
2005
2010
2015
2020
2025
Year

Tmax

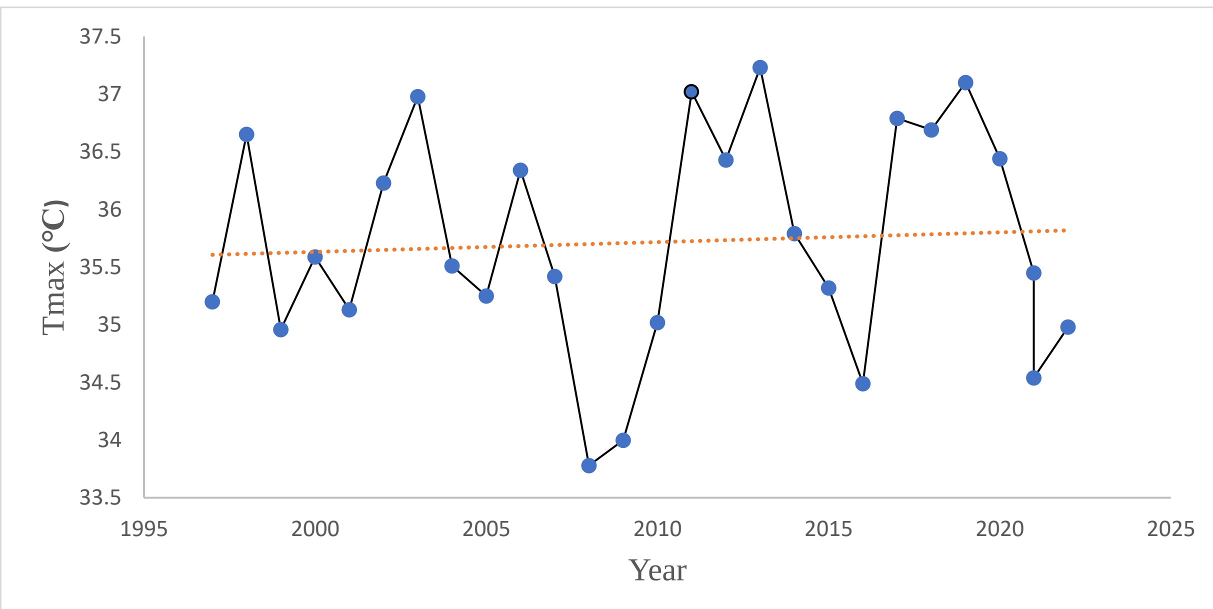
Tmax (°C)
37.5
37
36.5
36
35.5
35
34.5
34
33.5
1995
2000
2005
2010
2015
2020
2025
Year

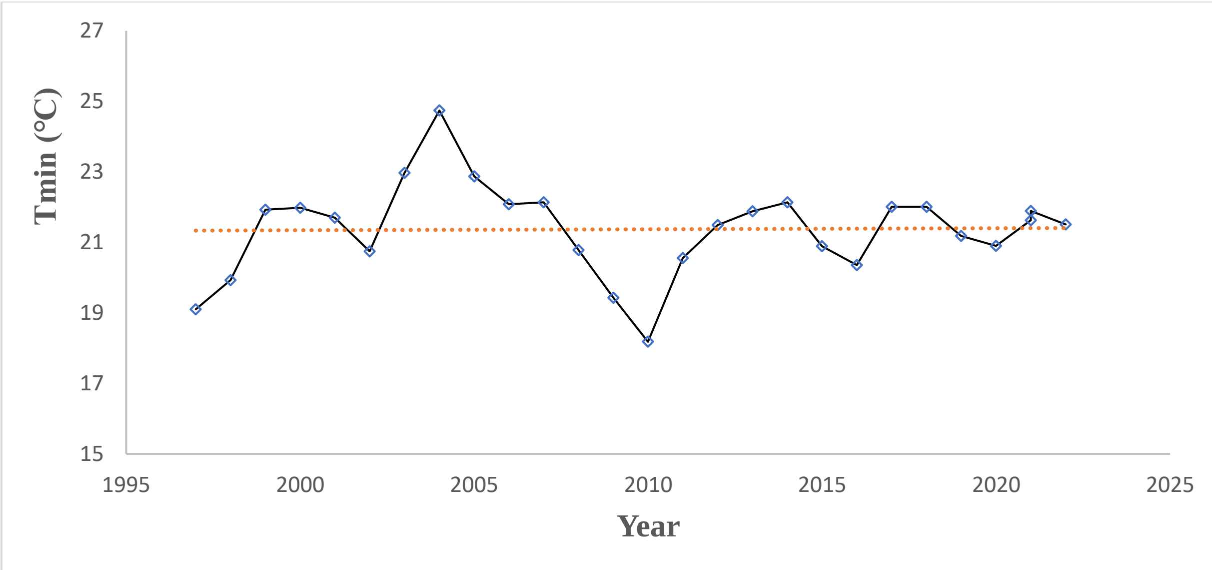

Tmin (°C)
27
25
23
21
19
17
15
1995
2000
2005
2010
2015
2020
2025
Year